THE SYNTHESIS, CHARACTERISATION AND APPLICATION OF PHOSPHORYLATED MULTIWALLED CARBON NANOTUBES FOR THE TREATMENT OF RADIOACTIVE WASTE

---

by

Nikiwe Mhlanga

Dissertation in fulfilment of the requirement for the degree

MASTER OF SCIENCE

in

CHEMISTRY

in the

FACULTY OF SCIENCE

of the

UNIVERSITY OF JOHANNESBURG

Supervisor	**:**	**Dr X.Y. Mbianda**
Co-supervisors	**:**	**Ms. K. Pillay**
	:	**Prof. W. Meyer**

DECLARATION

I hereby declare that this dissertation, which I herewith submit for the research qualification

MASTERS DEGREE IN CHEMISTRY

to the University of Johannesburg, Department of Chemical Technology, is, apart from the recognised assistance of my supervisors, my own work and has not previously been submitted by me to another institution to obtain a research diploma or degree.

_____ on this ____ day of _____

(Candidate)

_____ on this ____ day of _____

(Supervisor)

_____ on this ____ day of _____

(Co-supervisor)

_____ on this ____ day of _____

(Co-supervisor)

DEDICATION

This mileage is dedicated to my loving dad and mom Mr and Mrs D.B Mhlanga, my siblings (Mayibongwe, Sinenhlanhla, and Banele) and finally to my grandma (LaMamba). Profound gratitude boKhabako for believing in me always. These are the fruits of your true and unending love which you continuously shower me with. The warmth and sense of belonging I always feel whether I'm at home or not (you live in me).

"Ngiyanitsandza boKhabako Wabolanga"

Glory belongs to God, honour to my parents and the privilege was mine

ACKNOWLEDGEMENTS

Sincere appreciation to the following;

- The Lord almighty for giving me life and the privilege. Although He cannot be seen by naked eyes, He is all around me. He is visible in the blue skies, the ocean, the birds and all the beautiful creation especially the good people surrounding me. He kept me so I would not let go.
- My supervisors; Dr. X.Y. Mbianda, Ms. K. Pillay (University of Johannesburg) and Prof. W. Meyer (Necsa) for patience, guidance and inputs through-out the study.
- National research foundation (NRF), University of Johannesburg and Necsa for financial support.
- Sylva Olsen, A. Goede and J. Badenhorst from Necsa for their supervision in the extraction of uranium and iodine experiments at Necsa.
- Witwatersrand staff for help with the TEM, TGA, BET and Raman analysis.
- T.I. Nkambule, S.M. Mamba and M. Mahlambi for proofreading and assistance with the template
- My family; parents, aunts, uncles and siblings. For their love, prayers, support and encouragement. Love you tons.
- My best friends forever (BFFs); Mthaby, Njabuliso (MyD), Unathi and Phile. Thank you so much for the good times we shared. I will always hold on to the good memories. My pillars in time of distress and need. Thank you for making me laugh in the mist of challenges. Much love BFFs (family away from home)
- My colleagues and friends; the phosphorus group especially Martha Neosi (thank you for laughter and help in the laboratory) and all the postgraduate team.
- Prayer group; for the encouragement and prayers.

If it had not been for the *Lord* on my side, let "*Nikiwe Thembumenzi"* now say "Thank you so much to all of you"

CONFERENCES AND PUBLICATIONS

Conferences

- Mhlanga N., Mbianda X.Y. and Meyer W. *The synthesis and application of phosphorylated multiwalled carbon nanotubes in the treatment of radionuclear waste*. 1st annual SANHARP postgraduate conference. 23-25 August 2009. iThemba labs Cape Town. Oral presentation.

- Mhlanga N., Mbianda X.Y. Meyer W. and Goede A. *Synthesis Of multiwalled carbon nanotubes methylene dibutyl phosphate (MWCNTs-MDBP): characterisation and application in nuclear waste treatment.* 4th international conference on environmental effects of nanoparticles and nanomaterials. Austria. 6-9 September 2009. Poster presentation.

Publications

- Mhlanga N., Mbianda X.Y., Pillay K. and Meyer W. The synthesis of multiwalled carbon nanotubes methylene dibutyl phosphate (MWCNTs-MDBP). [In preparation for publication].

- Mhlanga N., Mbianda X.Y., Pillay K. and Meyer W. The synthesis of multiwalled carbon nanotubes tributyl phosphate polymer (MWCNTs-TBP), [In preparation for publication].

ABSTRACT

Radionuclides exist in the environment because of natural and human activities that are an essential part of our lives. Nuclear processing, medicinal applications (using isotopes) and electric power production by nuclear stations are few examples of human activities that result in production of radioactive waste (RAW). The nuclear power stations in our world have to store their waste in such a manner that the present and future generations are protected from harmful radiations and this is a challenge. Exposure to RAW can result in severe, diverse and irreversible consequences such as damage of the ecosystem, pollution, cancers, birth mutations, to mention just a few.

Solvent extraction (SE) technique is currently used to purify large volumes of secondary liquid waste before they are released to the environment or stored. However, even after the SE purification, highly radioactive liquid waste is given off. This highly radioactive liquid waste is solidified in a glass matrix (vitrification). In an attempt to reduce the disposal of large volumes of secondary RAW generated during the purification technology, this study was initiated to investigate the possibility of using multiwalled carbon nanotubes (MWCNTs) as part of the SE technique. As the main nuclear liquid extraction processes involve tributyl phosphate (TBP), the MWCNTs were linked to TBP, polymerised to give a MWCNTs-TBP polymer that was tested in the nuclear environment. This polymer should possess good chelating properties due to the inclusion of the phosphate and should be a good absorbent as MWCNTs are promising absorbent carbon materials. To test the hypothesis of the study MWCNTs-TBP polymer was tested for uranium extraction. The MWCNTs-TBP polymer gave a zero K_d value which indicates that the adsorption capacity of the polymer to remove radionuclides from waste streams was not successful. The MWCNTs were then tested for iodine-131 extraction whereby they were compared with single walled carbon nanotubes (SWCNTs) and double walled carbon nanotubes (DWCNTs). In this test SWCNTs gave a K_d value of 81694 mL/g which proved that they can be used in nuclear waste applications.

TABLE OF CONTENTS

Section ***Page***

Declaration i

Dedication ii

Acknowledgements iii

Conferences and publications iv

Abstract v

Table of contents vi

List of figures xi

List of schemes xiii

List of tables xiv

List of abbreviations xv

CHAPTER 1 : INTRODUCTION 1

1.1 Background 1

1.2 Problem statement 1

1.3 Justification 2

1.4 Objectives of the study 2

1.5 Dissertation outline 3

References: 4

CHAPTER 2 : LITERATURE REVIEW 6

2.1 Introduction 6

2.2 Radioactive waste 6

2.3 Classification of radioactive waste 7

2.3.1 High level waste (HLW) 7

2.3.2 Intermediate level waste (ILW) 7

2.3.3 Low level waste (LLW) 8

2.4 Techniques for radioactive waste treatment 8

2.4.1 REDOX process 8
2.4.2 Plutonium Uranium Redox Extraction (PUREX) 9
2.4.3 DIAMEX process 10
2.4.4 Trans Uranium Extraction (TRUEX) 11
2.4.5 TRAMEX 11
2.4.6 Separation by Phosphorus Extractants and aqueous Complexes (TALSPEAK) Process 12
2.4.7 Uranium Extraction (UREX) 13
2.5 Carbon nanotubes (CNTs) 14
2.5.1 Applications of CNTs 14
2.5.2 Synthesis of CNTs 15
2.5.2.1 Arc Discharge 15
2.5.2.2 Laser ablation 15
2.5.2.3 Chemical vapour deposition (CVD) 16
2.5.2.4 Nebulised Spray Pyrolysis (NSP) 16
2.5.2.5 Natural, Incidental and controlled flame environment 17
2.5.3 Purification of CNTs 17
2.5.4 Functionalisation of CNTs 18
2.5.4.1 Oxidation by acid treatment 19
2.5.4.2 Mechano-chemical modification 19
2.5.4.3 1,3-dipolar cycloaddition of Azomethine ylides 19
2.5.4.4 Electrochemical Modification (ECM) 19
2.5.4.5 Fluorination 20
2.5.4.6 Arylation and Alkylation of CNTs 21
2.5.4.7 Azide Photochemistry 21
2.6 Tributyl phosphate (TBP) 21
2.6.1 Background 21
2.6.2 TBP complexation mechanism 22
2.6.3 Characterisation Techniques for the Carbon nanotubes and phosphates 23
2.6.3.1 Scanning Electron Microscope (SEM) 23
2.6.3.2 Transmission Electron Microscope (TEM) 23
2.6.3.3 Fourier Transform Infrared Spectroscopy (FTIR) 23
2.6.3.4 Thermogravimetric Analysis (TGA) 24

2.6.3.5 Nuclear Magnetic Resonance (NMR) 24
2.6.3.6 RAMAN 24
2.6.3.7 Energy-dispersive X-ray Spectroscopy (EDX) 25
2.6.3.8 Brunauer Emmet Teller 25
2.6.4 Conclusion 25
References: 27

CHAPTER 3 : EXPERIMENTAL METHODOLOGY 35

3.1 Introduction 35
3.2 Chemicals and Reagents 35
3.3 Characterisation of Samples 35
3.3.1 Instrumentation 35
3.3.2 Preparation of samples for characterisation 36
3.3.2.1 Fourier Transform Infrared 36
3.3.2.2 Scanning Electron Microscope 36
3.3.2.3 Energy-dispersive X-ray Spectroscopy 36
3.3.2.4 Transmission Electron Microscope 36
3.3.2.5 Raman 37
3.3.2.6 Thermo Gravimetric Analysis 37
3.3.2.7 NMR 37
3.3.2.8 Brunauer Emmet Teller 37
3.3.2.9 UV-visible Spectrophotometer 38
3.3.2.10 Scanning X-ray photoelectron Spectroscopy (SXPS) . 38
3.4 Experimental Procedure 39
3.4.1 MWCNTs synthesis 39
3.4.2 Purification of the MWCNTs 40
3.4.3 Functionalisation of the MWCNTs 41
3.4.3.1 Oxidation of MWCNTs 41
3.4.3.2 Acylation and amidation of MWCNTs 42
3.4.3.3 Reduction of Amidated MWCNTs 43
3.4.4 Synthesis of phosphorylating reagents and Phosphorylation of MWCNTs 44
3.4.4.1 Synthesis of Dibutyl chlorophosphate 44

3.4.4.2 Synthesis of multiwalled carbon nanotube methylene Dibutylphosphate (MWCNTs-MDBP) 45
3.4.4.3 Chlorotributyl phosphate (Cl-TBP) synthesis 46
3.4.4.4 Synthesis of azido-tributyl phosphate (azido-TBP) 47
3.4.4.5 Synthesis of multiwalled carbon nanotubes-tributyl phosphate (MWCNTs-TBP) 48
3.4.4.6 Synthesis of MWCNTs-TBP polymer 48
3.4.5 Extraction of Uranium using pristine and functionalised MWCNTs 49
3.4.5.1 Procedure for determination of distribution co-efficient (Kd) values 49
3.4.5.2 Determination of the ratio of tracer distribution between the liquid phase and different MWCNTs samples by UV spectroscopy 50
References: 51

CHAPTER 4 RESULTS AND DISCUSSIONS 52

4.1 Introduction 52
4.2 Scanning Electron Microscope 52
4.3 Transmission Electron Microscope 54
4.4 Fourier Transform Infrared Spectroscopy 56
4.5 Raman 57
4.6 Thermo Gravimetric Analysis 59
4.7 Energy dispersive X-ray Spectroscopy 62
4.8 Scanning X-ray photoelectron Spectroscopy 65
4.9 Brunauer Emmet-Teller 66
4.10 Application of the MWCNTs samples in radionuclear waste treatment 67
4.11 Conclusion 71
References: 73

CHAPTER 5 CONCLUSIONS AND RECOMMENDATIONS 75

5.1 Conclusions 75

5.2 Recommendations 76

APPENDIX NMR AND FTIR SPECTRA 77

LIST OF FIGURES

Figure ***Description*** ***Page***

Figure 2.1: The PUREX process 10

Figure 2.2: The TRUEX process. 11

Figure 2.3: The TRAMEX process..... 12

Figure 2.4: The UREX process..... 13

Figure 2.5: Showing the SWCNT and MWCNT. 14

Figure 2.6: electrolytic cell used for ECM. 20

Figure 2.8: Tributyl phosphate..... 22

Figure 3.1: The experimental set up for MWCNTs synthesis by NSP 40

Figure 3.2: The soxhlet extractor..... 41

Figure 3.3: The set up used for synthesis of Dibutyl chlorophosphate 45

Figure 4.1: SEM images a) Pristine MWCNTs b) MWCNTs-COOH c) MWCNTs-CH_2OH d) MWCNTs-MDBP e) MWCNTs-TBP and f) MWCNTs-TBP polymer. 53

Figure 4.2: TEM images a) Pristine MWCNTs b) MWCNTs-COOH c) MWCNTs-CH_2OH d) MWCNTs-MDBP e) MWCNTs-TBP and f) MWCNTs-TBP polymer. 55

Figure 4.3: The FTIR spectra a) Pristine MWCNTs b) MWCNTs-COOH c) MWCNTs-CH_2OH d) MWCNTs-MDBP e) MWCNTs-TBP and f) MWCNTs-TBP polymer. 57

Figure 4.4: Raman a) pristine MWCNTs b) MWCNTs-COOH c) MWCNTs-CH_2OH d) MWCNTs-MDBP e) MWCNTs-TBP and f) MWCNTs-TBP polymer. 58

Figure 4.5: TGA for Pristine MWCNTs, MWCNTs-COOH, MWCNTs-CH_2OH MWCNTs-MDBP, MWCNTs-TBP and MWCNTs-TBP polymer. . 61

Figure 4.6: Derivatives plots for MWCNTs-TBP and MWCNTs-TBP polymer..... 61

Figure 4.7: EDX a) Pristine MWCNTs b) MWCNTs-COOH 63

Figure 4.8: a) EDX MWCNTs-MDBP b) MWCNTs-TBP c) MWCNTs-TBP polymer 64

Figure 4.9: SXPS for MWCNTs-MDBP. 65

Figure 4.10: SXPS for MWCNTs-TBP polymer 66

Figure 4.11: Eh-pH and uranium species distribution as a function on pH for oxidising-reducing conditions. 68

LIST OF SCHEMES

Scheme	Description	Page
Scheme 2.1:	The reaction pathway for the REDOX process.	9
Scheme 2.2:	Extraction of Uranyl nitrate by TBP	22
Scheme 3.1:	The summary of the methodology.	39
Scheme 3.2:	Reaction pathway for oxidation of MWCNTs.	42
Scheme 3.3:	The reaction pathway for acylation and amidation of MWCNTs	43
Scheme 3.4:	The reduction of amidated MWCNTs.	43
Scheme 3.5:	Reaction pathway for dibutyl chlorophosphate synthesis.	44
Scheme 3.6:	Reaction pathway for MWCNTs-MDBP synthesis.	46
Scheme 3.7:	Reaction pathway for Cl-TBP	47
Scheme 3.8:	Reaction pathway for azido-TBP.	47
Scheme 3.9:	Reaction pathway for synthesis of MWCNTs-TBP.	48
Scheme 3.10:	Reaction pathway for polymerisation of MWCNTs-TBP.	49

LIST OF TABLES

Table ***Description*** ***Page***

Table 2.1: Impurities and their possible purification techniques 18

Table 4.1: Index for the graphitisation degree of the MWCNTs..... 59

Table 4.2: Thermal stability of the pristine MWCNTs, MWCNTs-COOH, MWCNTs-CH_2OH, MWCNTs-MDBP, MWCNTs-TBP and MWCNTs-TBP polymer..... 62

Table 4.3: BET results for the different MWCNTs samples 67

Table 4.4: The K_d values of uranium extraction by MWCNTs samples 70

Table 4.5: The K_d values for iodine extraction by the Carbon materials 71

LIST OF ABBREVIATIONS

AHA	Acetohydroxamic acid
Azido-TBP	Azido-tributyl phosphate
BET	Brunauer emmet teller
CEA	Commissariat energie atomic
Cl-TBP	Chloro-tributyl phosphate
CMPO	Octyl(phenyl)-N,N-dibutylcarbamoly-methylphosphine oxide
CNTs	Carbon nanotubes
CVD	Chemical vapour deposition
D-band	Dis-order band
DMF	Dimethyl formaldehyde
DTPA	Diethylenetriamine pentaacetic acid
DWCNTs	double walled carbon nanotubes
ECM	Electrochemical modification
EDX	Energy dispersive X-ray spectroscopy
EtN_3	Triethyl amine
FTIR	Fourier transform infrared spectroscopy
G-band	graphite band
G`-band	Second order Raman scattering from D-band vibrations
GW_e	Gigawatts electric
HDEHP	Di(2-ethylhexyl)phosphoric acid
HLW	High level waste
HSVM	High speed vibration mill
ILW	Intermediate level waste

K_d	The ratio of adsorbate adsorbed quantity per unit mass of a solid to the amount of the adsorbate that was present in the solution
LLW	Low level waste
MA	Minor actinides
MIBK	Methylisobutyl ketone
MWCNTs	Multiwalled carbon nanotubes
MWCNTs-COOH	Oxidised multiwalled carbon nanotubes
MWCNTs-CH_2OH	Multiwalled carbon nanotubes linked to hydroxyl functions
MWCNTs-MDBP	Multiwalled carbon nanotubes-methylene dibutyl phosphate
MWCNTs-TBP	Multiwalled carbon nanotubes-tributyl phosphate
NMR	Nuclear magnetic resonance
NORM	Naturally occurring radioactive material
NSP	Nebulised spray pyrolysis
p-MWCNTs	Phosphorylated multiwalled carbon nanotubes
PTFE	polytetrafluoroethylene
PUREX	Plutonium uranium extraction
RBM	Radial breathing mode
RAW	Radioactive waste
SE	Solvent extraction
SEM	Scanning electron microscope
SCCM	Standard cubic centimetres per minute
SNF	Spent nuclear fuel
SXPS	Scanning X-ray photoelectron spectroscopy
SWCNTs	Single walled carbon nanotubes
TALSPEAK	Separation of phosphorus extractants and aqueous complexes

TBP	Tributyl phosphate
TDI	Toloylene -2,4-diisocyanate
TEM	Transmission electron microscope
TGA	Thermogravimetric analysis
THF	Tetrahydrofuran
TRUEX	Trans uranium extraction
UREX	Uranium extraction

CHAPTER 1

INTRODUCTION

1.1 Background

Radioactive waste (RAW) is a type of waste which contains components that are unstable due to radioactive decay.[1] This waste is generated from man-made processes such as industrial, domestic, agricultural and commercial activities.[2] It also occurs naturally and is refereed to as naturally occurring radioactive material (NORM).[1] It can exist as either a solid or a liquid state.[2] Exposure to RAW causes air and water pollution, which can have a negative effect on the health of human beings. This is because of its toxicity, physical and chemical properties.[2] Therefore, this waste requires proper management to ensure protection of human beings and the environment.[1] To guarantee safety for the living organisms the treatment, proper handling and storage of RAW is fundamental. The type of radiation found in different types of RAW differs and it determines the handling, treatment, transportation and storage of the waste.

1.2 Problem statement

Treatment of RAW entails recovering the radionuclides and thereby reducing the radioactivity levels of the waste. Several techniques, such as precipitation, co-precipitation and ion-exchange chromatography have been used for the treatment of RAW.[3] The solvent extraction (SE) technique, which separates and reduces amount of radionuclides has been in use by nuclear facilities.[4] This is because the SE technique is used for industrial large-scale applications due to its simplicity[3] and amenability to finite stage mass transfer unit operations.[5] However, the SE technique generates volumes of secondary waste by the radiolytic degradation of extractants.[3,6,7] Nuclear power stations uses deep geological disposal facilities for the disposal of RAW.[8] The liquid RAW is solidified into a matrix (vitrification) before storage. This project aims at reducing the secondary

waste by using the phosphorylated multiwalled carbon nanotubes (p-MWCNTs) as an extractant in the SE technique. MWCNTs have striking and unique features that make them suitable candidates for the adsorption of radionuclides. MWCNTs for instance, have a petite hollow size, a large surface area, high mechanical strength and electrical conductivity.[9,10,11] Several experiments on adsorption using MWCNTs have been reported. For example, CNTs have been used as adsorbents for inorganic and organic pollutants such as Cd,[12] Cu(II), Pd(II), Zn(II), Ni(II) and Co(II),[13] atrazine and simazine (herbicides).[14]

1.3 Justification

Purification of the RAW generated from nuclear facilities by the p-MWCNTs will reduce the radioactivity level of the RAW by recovering more radionuclides; hence RAW risk to the environment is reduced. Contaminated p-MWCNTs will be disposed as solid waste. Incorporation of the solid contaminated p-MWCNTs into the matrix by vitrification will enhance the properties of the matrix before it is stored in deep geological sites.

1.4 Objectives of the study

This project is undertaken to synthesise a polymer of p-MWCNTs as an extractant for the SE technique. Disposal of solid RAW with reduced radioactivity is anticipated.

The objectives of the study are as follows;

- To synthesise multiwalled carbon nanotubes
- To purify and functionalise the synthesised multiwalled carbon nanotubes
- To synthesise phosphorylating reagents
- To phosphorylate and polymerise MWCNTs using the phosphorylating reagents (tributyl phosphate and methylene dibutyl phosphate)

- To apply the phosphorylated MWCNTs (p-MWCNTs) in the treatment of RAW

1.5 Dissertation outline

The dissertation outline gives a summary of what is discussed in chapter 2 to 5.

Chapter 2 *(Literature review)*

In this chapter, RAW is discussed i.e. its definition, origin, types and treatment. Chapter 2 tackles the advantages and disadvantages of the treatment techniques. The uses of CNTs that are capable candidates in solving the problems associated with the treatment of RAW are discussed. Their synthesis, purification, functionalisation, application and characterisation techniques used are elaborated.

Chapter 3 *(Experimental procedures)*

This section gives an insight of the experimental procedures that were employed to attain the objectives of the study.

Chapter 4 *(Results and discussion)*

This chapter presents and discusses the results of the study. Synthesis and functionalisation of MWCNTs and the application in the treatment of RAW is reported in this section.

Chapter 5 *(Conclusion and recommendations)*

Conclusions based on the interpretation of the results from chapter 4 are drawn. Recommendations for future work are brought forward.

References:

1. P.A. Baisdea and G.R. Choppin. Nuclear waste management and the nuclear fuel cycle, in Radiochemistry and Nucl. Chem, [Ed. Sandor Nagy], in Encyclopedia of life support systems (EOLSS), Developed under the Auspices of the UNESCO, EOLSS Publishers, Oxford, UK, [http://www.eolss.net]. (2007). (Accessed 18 October 2008)

2. L. Bredenham, H.O. Fourie and K. Langaman. Minimum requirements for the handling, classification and disposal of hazardous waste. 2nd ed. Published by department of water affairs and forestry, Pretoria. (1998)

3. C.K Raju and M.S. Subramania. Sequential separation of lanthanides, thorium and uranium using novel phase extraction method from high acidic nuclear waste. *Journal of Hazardous Material*. **145** (2007) 315-322.

4. H. M. Freeman and E.F. Harris. Hazardous waste remediation. Innovative treatment technologies. Technomic publishing co, INC, USA. (1995) 157.

5. T.A. Todd; T.A. Batcheller; J.D. Law and R.S. Bobst. Cesium and strontium separation technologies literature review. Idaho National engineering and Environmental laboratory Bechtel BW XI, Idaho, LLC (INEEL). (2004).

6. A. Zhang; C. Xiao; E. Kuraoka and M. Kumagai. Molecular of novel macroporous silica-based impregnated polymeric composite by tri-n-butyl phosphate and its application in the adsorption for some metals contained in a typical simulate HLLW. *Journal of Hazardous materials*. **147** (2007) 601-609.

7. P.W. Naik; P.S. Shami; S.K. Misra; U. Jambunathan and J.N. Mathur. Use of organophosphorus extractants impregnated on silica gel for the extraction chromatographic separation of minor actinides from high level waste solutions. *Journal of Radionalytical and Nuclear Chemistry*. **257** (2003) 327-332.

8. Atomic Energy Licensing Board (AELB). Radioactive waste management. National committee for the certification of radiation protection officer. http://www.aelb.gov.my/events/lamanweb2/docs/7%20%new%20elements%20In%20AELB`s%20insection%20(2).pdf. (accessed 27 February 2009)

9. C. Chen; J. Hu; D. Shao; J. Li and X. Wang. Adsorption behavior of multiwall carbon nanotubes/ iron oxide magnetic composites for Ni(II) and Sr(II). *Journal of Hazardous Material*. **64** (2009) 923-928.

10. C. Chen; J. Hu; D. Xu; X. Tan; Y. Meg and X. Wang. Surface complexation modeling of Sr(II) and Eu (III) adsorption onto oxidized multiwall carbon nanotubes. *Journal of Colloid and Interface Science*. **322** (2008) 33-41.

11. J. Hu; C. Chen; X. Zhu and X. Wang. Removal of chromium from aqueous solution by using oxidised multiwalled carbon nanotubes. *Journal of Hazardous Material*. **162** (2009) 1542-1550.

12. J. Xiao; Q. Zhou and H. Bai. Application of multiwalled carbon nanotubes treated by potassium permanganate for determination of trace cadmium prior to flame atomic absorption spectroscopy. *Journal of Environmental Sciences*. **19** (2007) 1266-1271.

13. M. Tuzen; K.O. Saygi and M. Soylak. Solid phase extraction of heavy metal ions in environmental samples on multiwalled carbon nanotubes. *Journal of Hazardous Materials*. **152** (2008) 632-639.

14. Q. Zhou; J. Xiao; W. Wang; G. Liu; Q. Shi and J. Wang. Determination of atrazine and simazine in environmental water samples using multiwalled carbon nanotubes as the adsorbents for preconcentration prior to high performance liquid chromatography with diode array detector. *Talanta*. **68** (2006) 1309-1315.

CHAPTER 2

LITERATURE REVIEW

2.1 Introduction

This chapter discusses matters pertaining to radioactive waste; it explains what radioactive waste is, its classification and the different techniques used in its treatment. It also tackles the disadvantages of the treatment techniques and carbon nanotubes are introduced as the possible solution for the problem of disposal of volumes of liquid secondary waste. Synthesis, purification and functionalisation of the carbon nanotubes are highlighted in this section.

2.2 Radioactive waste

Radioactive waste (RAW) is produced as a result of both natural and human (nuclear processing, medicinal applications) activities.[1] RAW requires proper management to ensure the safety of the environment. This is because it consists of components that are not stable because of radioactive decay.[1] Nuclear processing is of great importance today as about 16% of the world's total electric power is generated from nuclear power stations.[2] The electric power is generated by 438 Nuclear power stations and approximately 351 gigawatts electric (GW_e) is produced.[3] Since the world's population and the standard of living are increasing everyday, and even rural settlements are now depending on electricity for various activities, nuclear power stations are bound to increase to meet the world's demand of power. However, the nuclear power stations are faced with a challenge of managing the RAW. Generally, three distinct strategies can be used to manage RAW.[4] These include:

- Treat and contain – This strategy is used for high-hazard waste. The RAW is treated and encapsulated for disposal. The encapsulated RAW is then isolated in an appropriate environment (deep geological storages)

where it doesn't come into contact with the environment except for the one that it is stored in.[4]

- Dilute and disperse – the RAW level of radioactivity is lowered to acceptable levels directly or by treatment. It is then discharged to the environment. This strategy is used for low-hazard waste.[4]

- Delay to decay – the RAW is stored and allowed to decay to acceptable levels of radioactivity before being dispersed to the environment.[4]

2.3 Classification of radioactive waste

Several criteria have been used to classify RAW. These include level of radioactivity, type of radiation emitted (gamma, beta), half life and physical characteristics (solid, liquid and gaseous state).[1] For this study, the level of radioactivity will be used to classify RAW as follows:

2.3.1 High level waste (HLW)

This type of waste is made up of constituents with very high radioactive levels. HLW result straight from production of nuclear materials, reprocessing of spent nuclear fuel (SNF) and waste produced directly in reprocessing. This waste can be treated and contained before being isolated into an appropriate environment.[5]

2.3.2 Intermediate level waste (ILW)

The levels of radioactivity are lower compared to those of HLW. However, they still need proper management. Sludge from spent fuel cooling, storage areas and cleaning materials are examples of ILW. ILW is divided to short-lived solid and long-lived waste. The short-lived solid can be managed by the delay to decay technique whereas the treat and contain technique is preferred for the long live waste. ILW constitutes about 4% of all RAW.[1]

2.3.3 Low level waste (LLW)

The radioactivity level is lower as compared to the HLW and ILW and unlike the two, LLW does not require shielding during transportation and handling which proves that the level of radioactivity is lower.[1] LLW is generated from medical and research activities, uranium enrichment processes, reactor operation, isotope production. LLW is found in materials incidental to and contaminated during the handling and transportation of RAW such as clothing, paper and glass.[6] Delay to decay and dilute to disperse are proper techniques for handling this type of waste.[1] The volume of the LLW is reduced by incineration before disposal. LLW constitutes about 90 % of RAW but only 1% is associated with radioactivity.[1] Nevertheless, traces of long live radionuclides can be found in the LLW and therefore disposal in near the surface is commonly used.[1]

2.4 Techniques for radioactive waste treatment

Several techniques have been used in the treatment of RAW. RAW is treated to reduce the level of radioactivity and to recover some of the radioactive element e.g. uranium and plutonium are recycled.[7] Precipitation or co-precipitation which was initially used for RAW treatment was mainly involved with the removal of uranium and plutonium from the radioactive fission and activated products.[1] However, co-precipitation of cesium and strontium by this technique resulted in the developments of alternative methods.[7]

Solvent extraction (SE) processes, were developed for the treatment of RAW. The SE technique is simple, affordable and can be used for large-scale application because of its amenability to finite-stage mass transfer unit operations.[7] The following SE processes are currently used in the nuclear industry;

2.4.1 REDOX process

The REDOX process was the first SE technique used and methylisobutyl ketone (MIBK) or hexone were used as the extractant.[8] Uranium and plutonium were removed from the oxidising solution by the extracting solvent used.[9] The REDOX

process downfall was brought about by the degradation of hexone in the nitric acid solution.[8] **Scheme 2.1** gives the REDOX process equation.

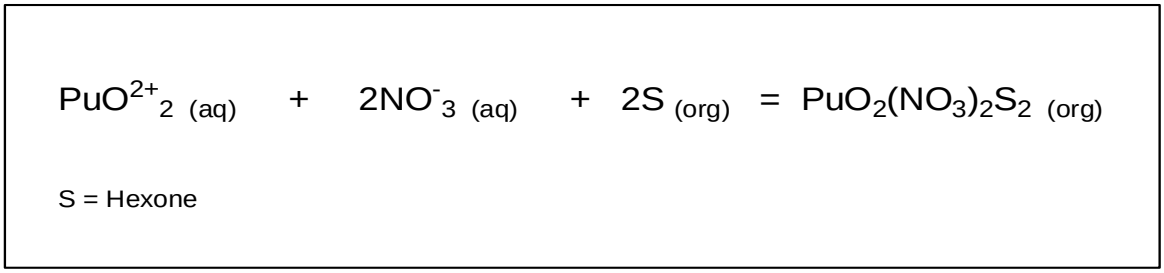

Scheme 2.1: The reaction pathway for the REDOX process.[9]

2.4.2 Plutonium Uranium Redox Extraction (PUREX)

The PUREX process replaced the REDOX process. Since its discovery, the PUREX process is still used internationally by most nuclear power stations even to date. The extracting solvent used in PUREX is tributyl phosphate (TBP), which is dissolved in kerosene. This technique removes UO^{2+}_2 and Pu^{4+} from RAW solutions.[1]

This process generates HLW that contains minor actinides (MA) and small amount of unrecovered uranium and plutonium. Several methods can be used to store the HLW but the most acceptable one is vitrification. In vitrification, the RNW is incorporated into a crystalline or glass matrix. The matrix is then deposited in deep geological repositories.[9] Additional methods like ion exchange processes can be used to aid the PUREX to make sure there is sufficient separation of certain fission products from the waste. A good example is the removal of ^{137}Cs from waste streams using ion exchange chromatography.[1] **Figure 2.1** shows how the PUREX process operates.

Although the PUREX process is used in the re-processing of nuclear fuel the use of TBP as an extracting reagent has drawbacks associated with the radiolytical degradation of the TBP.[2]

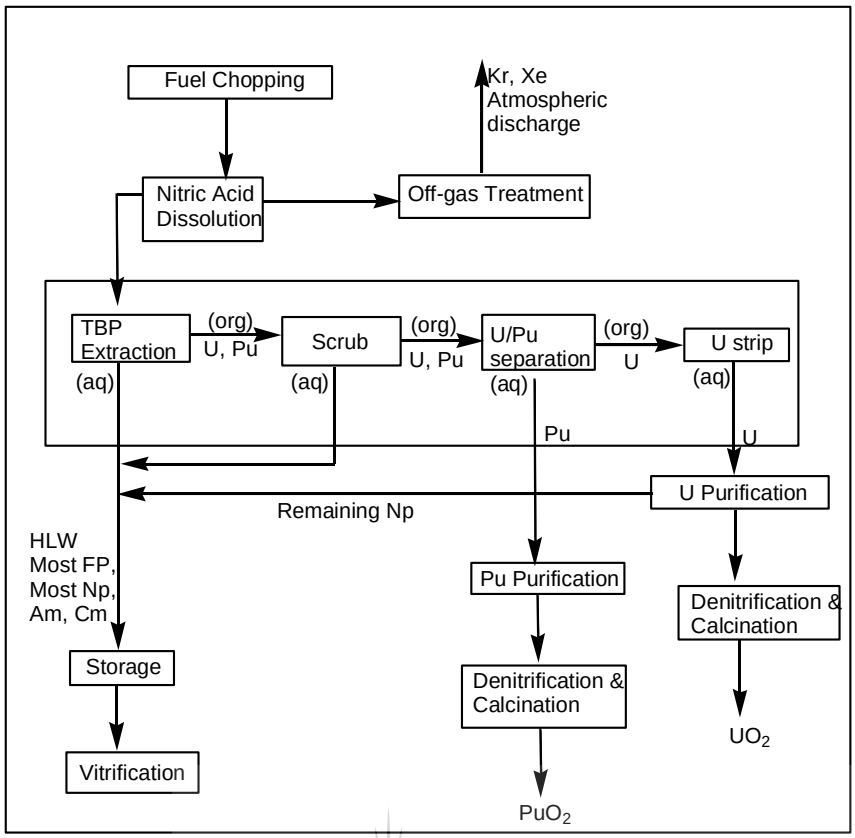

Figure 2.1: The PUREX process.[1]

2.4.3 DIAMEX process

Commissariat Energie Atomic (CEA) from France developed the DIAMEX process.[2] A research group programme by the European Union modified it to increase the removal of actinide elements from fission products.[2] A diamide such as N,N`-dimethyldiocytyhexyloxethylmalonamide is used as the extracting solvent.[3] In this process, the disposal of secondary waste is reduced because the extracting reagent used is completely incinerable.[2] However, large quantities of the extracting reagent have to be used for the extraction to be efficient. This is because they are not organophosphorus compounds.[3] Using p-MWCNTs as extracting reagents as opposed to the diamide will avoid use of large amount of extracting reagent because the MWCNTs will be linked to an organophosphorus compound.

2.4.4 Trans Uranium Extraction (TRUEX)

The TRUEX process was developed in the USA, Argonne National laboratory.[2] The main aim of the TRUEX process is to separate the transuranic elements from the acid HLW solution from the PUREX process.[1] Octyl(phenyl)-N,N-dibutylcarbamoly-methylphosphine oxide (CMPO) which is dissolved in an alkaline solvent is used as the extracting solvent. The TRUEX process is used to treat the HLW from the PUREX process.[1] During this process, plutonium and uranium are recovered but the tri- and tetra actinides are not separated from the lanthanides fission products.[8] **Figure 2.2** show the TRUEX process.

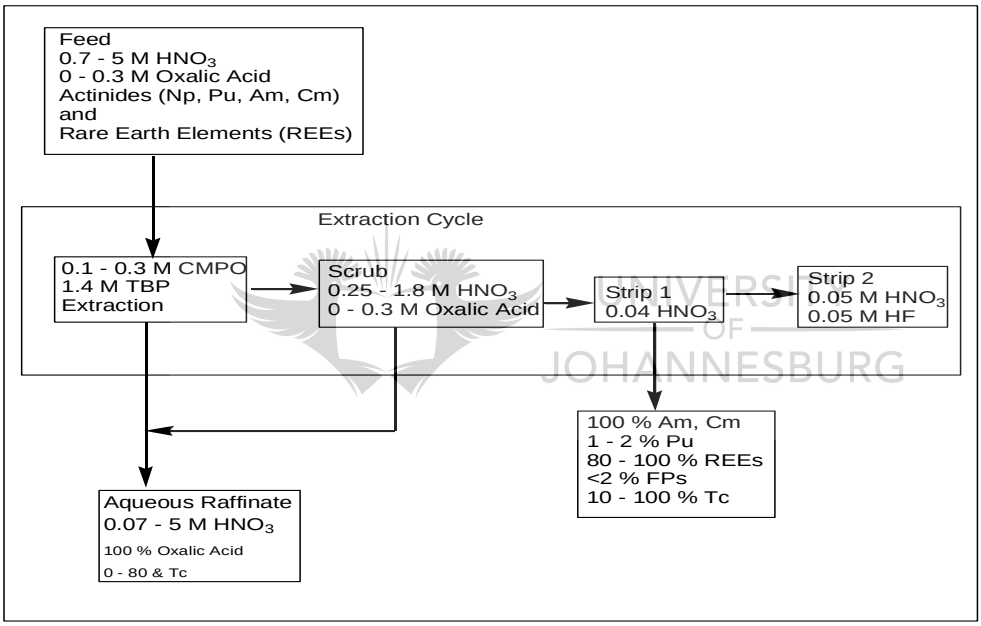

Figure 2.2: The TRUEX process.[1]

2.4.5 TRAMEX

The TRAMEX process separates the tri- and tetra-actinides from the lanthanides fission products. The liquid cation exchangers such as trialkyamines and tetraalkyammonium salts are used as extractant.[1] These extractants are dissolved in organic solvents to enhance the selectivity in the separation of the tri and tetra-actinides from lanthanides fission products. The aqueous nitrate solution from the PUREX process is treated to change it into a chloride feed solution. This

treatment is then followed by the separation of the tri- and tetra-actinides that is accomplished by the use of a solution with high chloride concentration.[9] However, there is a concern brought about by the use of concentrated chloride which is corrosive therefore requiring special processing units.[10] **Figure 2.3** elaborates on how the process works.

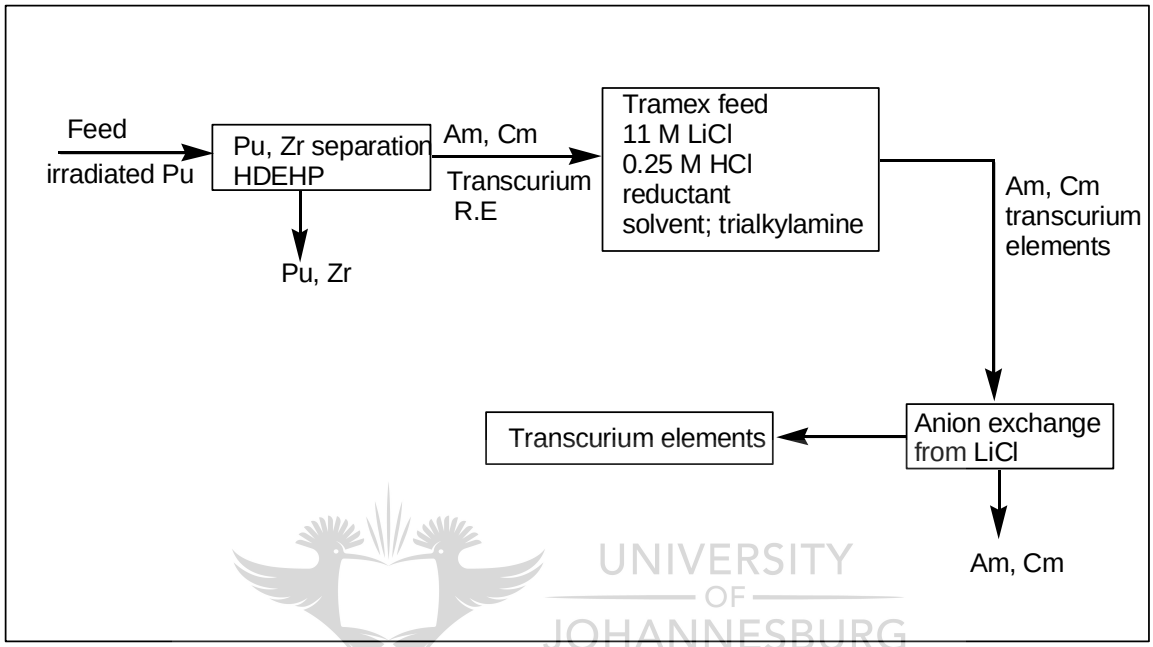

Figure 2.3: The TRAMEX process.[9]

2.4.6 Separation by Phosphorus Extractants and aqueous Complexes (TALSPEAK) Process

This process uses di(2-ethylhexyl) phosphoric acid (HDEHP) as an extracting solvent, this is shown in the first part of **Figure 2.3**. This process is made up of two versions that are the normal and the reverse version. In the normal version trivalent lanthanides are extracted using HDEHP from aqueous solution of both lactic and diethylenetriamine pentaacetic acid (DTPA) at pH 2.5 to 3.0. The reverse version, HDEHP extracts both actinides and lanthanides with subsequent stripping of the actinides into an aqueous phase containing lactic acid and DTPA.[11]

2.4.7 Uranium Extraction (UREX)

The UREX process is the variation of the PUREX process and just like the latter, it uses TBP as an extracting solvent. However, it differs from the PUREX in the sense that uranium is extracted at a high separation factor in one extraction cycle.[8] During the treatment process, the complexant acetohydroxamic acid (AHA), is added to the dissolver solution. This suppresses plutonium extraction and retains certain fission products thus avoiding contamination of the organic phase.[9] **Figure 2.4** explains how the UREX process operates.

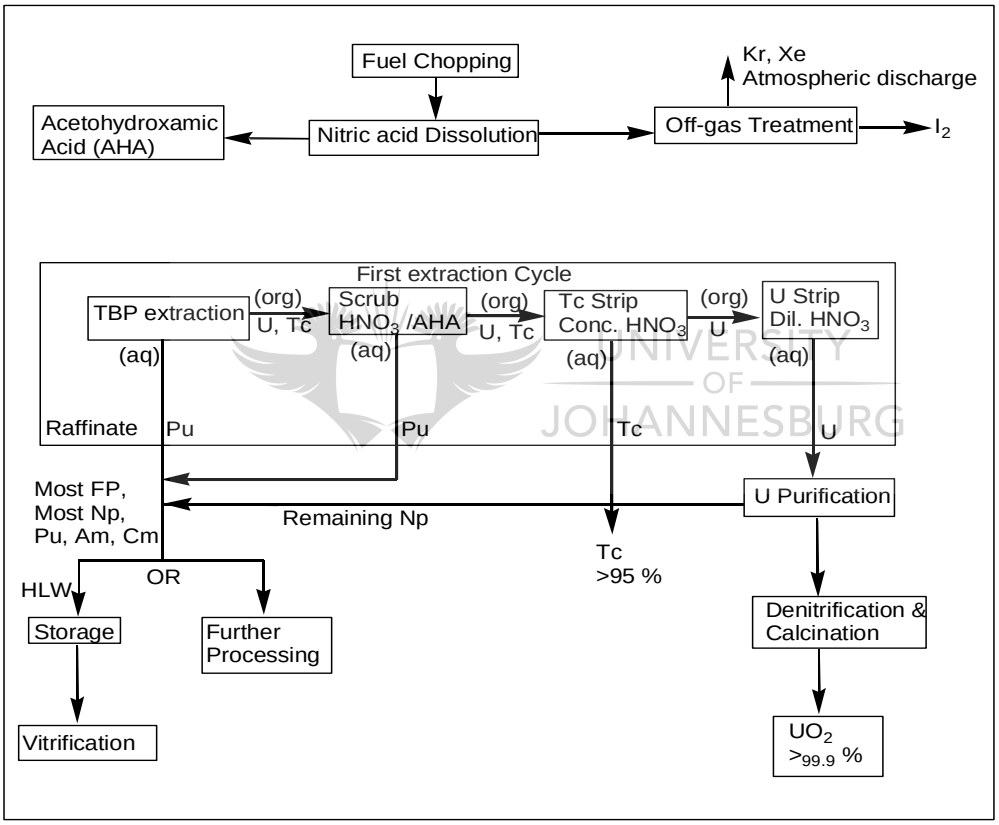

Figure 2.4: The UREX process.[1]

Although the SE technique is the driving force for the reprocessing, it also has a crucial problem as it generates liquid secondary waste that has high, long lasting radioactivity.[12] This waste can result in contamination of the environment. For example, in Russia contamination of the Yenisey River has been reported.[13]

2.5 Carbon nanotubes (CNTs)

CNTs are large molecules of pure carbon which are made up of rolled graphene sheets thus forming a cylindrical shape. Their diameter goes up to 100 nm and their length is in the size of the micrometer.[14] CNTs are classified as either single or multiwalled depending on the number of rolled graphene sheets they have. The single walled (SWCNTs) consist of only one sheet of graphite whereas the multiwalled carbon nanotubes (MWCNTs) are made up of more than one layer of graphene sheets.[15] **Figure 2.5** shows the SWCNT and MWCNT. CNTs have gained more interest from researchers because of their unique mechanical, chemical, thermal and optical properties.[16]

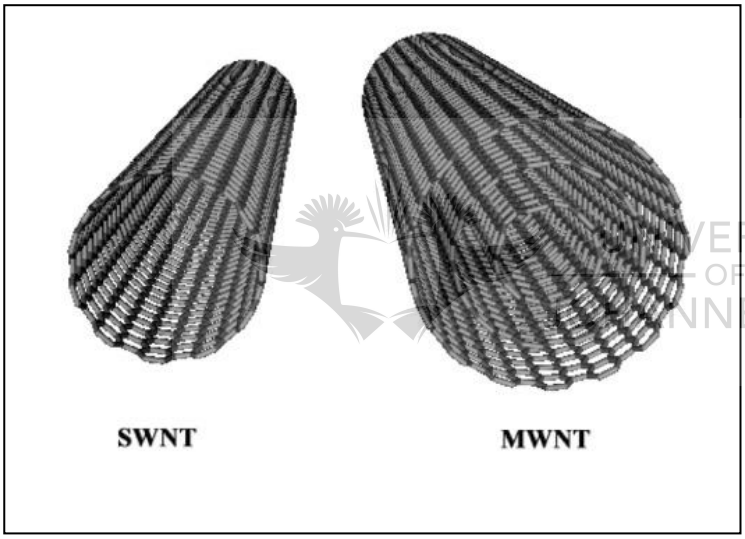

Figure 2.5: Showing the SWCNT and MWCNT.[17]

2.5.1 Applications of CNTs

CNTs have gained popularity since their discovery and they possess the ability to be applied in numerous scientific fields. These carbon materials have and are bringing improvement to our environment. They are used either as modifiers or in production of new compounds such as antimicrobial agents, environmental sensors, composite fibres and metal pre-concentration.[18]

MWCNTs have been used in water treatment for various purposes. They have been used in the removal of inorganic pollutants such as Ni (II), Am (III) and Cr (VI).[19] Heavy metals such as Zn (ll), Cd (ll) and Pb (ll) have been monitored by the use of these carbon allotropes.[20] Xiao *et al* (2007) used the MWCNTs as solid phase adsorbent for cadmium.[21] Oxidized CNTs have been used for removal of Sr(II) and Eu(III) where they showed greater adsorbent potential than other carbon materials they were compared with including: granular activated carbon, power activated carbon and fly ash.[22] The CNTs have also proven to have a greater adsorption capacity than activated carbon when they were used to adsorb H_2 and other gases.[23] However, no work has been reported on the application of phosphorylated MWCNTs in the treatment of RAW.

2.5.2 Synthesis of CNTs

Several techniques are used for the synthesis of CNTs and these include; arc discharge, laser ablation, chemical vapour deposition (CVD) and nebulised spray pyrolysis.

2.5.2.1 Arc Discharge

In 1991 Iijima intending to synthesise fullerenes using arc discharge discovered CNTs in the carbon soot of the graphite electrodes which were used for the synthesis.[24] In 1992 the first macroscopic CNTs were synthesized using Iijima technique by the researchers from NEC`s fundamental Research Laboratory.[25] The arc discharge is used till today for the syntheses of both single and multi walled CNTs.

2.5.2.2 Laser ablation

Richard Smalley and co-workers at the Rice University discovered the synthesis of CNTs by this technique coincidentally. While they were producing metal molecules by blasting metals using laser, they heard of iijima`s discovery, and they substituted the metal by graphite to synthesise CNTs.[26] To synthesise SWCNTs they used a composite of graphite and metal catalyst particles.[27] This technique

as compared to arc discharge produces better quality, high yield and allows control of growth conditions.[28]

2.5.2.3 Chemical vapour deposition (CVD)

This technique was used in 1993 although it was discovered back in 1959.[29,30] In 2007 researchers from the University of Cincinnati synthesised 18 mm long and aligned CNTs using the first-nano ET3000 carbon nanotubes growth system.[31]

A substrate is prepared using a metal catalyst which could be nickel, cobalt, iron or a combination of the metals. The size of the metal used influences the diameter of the CNTs.[32,33] Therefore if CNTs of bigger diameter is to be produced a metal of bigger size should be used to make the substrate and vice versa.[32] The set up for CVD is made up of a tubular furnace where a quartz tube is inserted. The substrate that is in a feedstock is introduced to the quartz tube by a flow of an inert gas which can be argon. Gas flow is switched to the feedstock for the specific growth period after which it is switched back to the inert gas while reactor is cooled down.[34] CVD is a promising technique for industrial scale production and therefore it has gained massive popularity. CVD allows the growth of CNTs in a desired substrate that makes it distinct from the other techniques and so far it is the only method producing vertically aligned CNTs.[31] More research is still ongoing to improve the CVD technique, in 2007 researchers from Meijo university developed CVD method for the synthesis of CNTs from camphor.[35] To prove the reliability of the CVD, it is currently used by several companies to synthesise CNTs in bulk, the companies include; Nanolab, Bayer, Arkema, Nanocyl, Nanothinx, hyperion catalysis, Mitsui and Showa Denko.[31]

2.5.2.4 Nebulised Spray Pyrolysis (NSP)

Spray pyrolysis is a modified version of CVD. It is a promising technique in the production of industrial scale, graphitised and well aligned MWCNTs at a lower cost.[36] This technique provides a continuous deposition of the CNTs throughout the synthesis cycle. In summary, a solution of the reactants is put into an atomization chamber connected to an oscillator. The power source is switched on

and the solution is atomized by the spray and carried by the carrier gas as vapour to a furnace that is heated to a certain temperature. The furnace is endowed with a quartz tube where the deposition of the CNTs takes place.[37]

2.5.2.5 Natural, Incidental and controlled flame environment

Burning of methane,[38] benzene[39], ethylene which can happen naturally can result in the production of CNTs.[40] CNTs can also be found from indoor to outdoor soot resulting from natural and propane gas.[41] However, these natural incidences are not reliable because they are not controllable and they produce CNTs which are not uniform therefore researchers find it hard to use them for research. Nevertheless, Nano-C, Inc of Westwood, Massachusetts is synthesising flame SWCNTs.[31]

2.5.3 Purification of CNTs

Purification as defined by the Oxford advanced English Learner's dictionary is to remove a pure form of a substance from other substances which contains it. During the synthesis of CNTs as described above, many chemicals are used as either carbon source or catalyst and these chemicals are not used up completely. Therefore, they remain with the synthesised CNTs as impurities. For the synthesised CNTs to be used for various applications they have to be purified. The impurities that are removed by purification could be the following: graphitic nano-particles, amorphous carbon, fullerenes, poly-aromatic hydrocarbons and catalyst materials such as metal catalyst.[42] The removal of the impurities is depended on two aspects which are: firstly, the characteristic of the impurities for instance their reactivity; and secondly, the stability of the nano-particles.[42] For example in a case where SWCNTs will have to be heated to a temperature above 1500 °C to remove a metal catalyst, the tubes can collapse due to the high temperature.[43] Removal of the impurities could be achieved either by using chemical or physical methods or by a combination of the two.[42] **Table 2.1** summarises the possible purification techniques for CNTs.

Table 2.1: Impurities and their possible purification techniques

Impurities	Purification Techniques
Graphitic nano-particles	Oxidation (dehydrogenation) – chemical.[42]
Amorphous carbon	Burning in air – physical.[44] Oxidation and hydrogenation – chemical.[45] Use of suitable chemical (H_2O_2, $HClO_4$, $KMnO_4$) – chemical.[45]
Fullerenes	Soxhlet extraction – chemical.[44]
Catalyst metal	Acid treatment – chemical.[46] Ultrasonic bath – physical.[43]
Catalyst support	Sonication, sedimentation and decantation – physical.[47]

2.5.4 Functionalisation of CNTs

Insolubility of the CNTs in most common solvents hinders their application in various fields.[48] Functionalisation enhances the solubility of the CNTs and their application in the different fields is accessible.[48] The functionalisation of CNTs has opened a completely new and promising era in their applications and development, for example, they can be bonded to a compound forming a polymer that possesses both CNTs good properties and those of the compound.[49]

Functionalisation of CNTs can be achieved by either indirect or direct attachment of the functional groups to the surface of the tubes.[50] The latter has the following examples; hydrogenation,[51] fluorination,[52] 1,3-dipolar cycloaddition[53] and interaction of CNTs with aniline,[54] nitrenes,[50] carbenes[50] and radicals[50]. The different methods used to modify CNTs are discussed in the following section.

2.5.4.1 Oxidation by acid treatment

To functionalise CNTs with carboxylic functions, several types of acids which are either a mixture of H_2SO_4/HNO_3 (3:1),[55] HNO_3 and HCl,[56] mixture of H_2SO_4 and H_2O_2[57] and other acids can be used. Acid treatment does not only generate carboxylic functions, it also purifies the CNTs.[58] However, acid treatment also opens the ends and shortens the CNTs.[15]

2.5.4.2 Mechano-chemical modification

For this modification, a high-speed vibration mill (HSVM) is used to produce pressure resulting in a chemical reaction. Functional groups such as carbonyl, chlorine, thiol and amine can be attached to the CNTs.[59] Mechano-chemical modification can be performed under wet or dry conditions depending on whether a solvent is used or not. The dry phase reaction is suitable for SWCNTs where KOH is reacted with the CNTs to form hydroxyl functions on to the surface of the CNTs at room temperature. For MWCNTs, the dry phase is not functional and therefore, the wet phase is used.[50,51]

2.5.4.3 1,3-dipolar cycloaddition of Azomethine ylides

Prato *et al* (2002)[53] developed a covalent functionalisation technique based on 1,3-dipolar cycloaddition of azomethine ylides. The azomethine ylides are generated or derived from the condensation of an alpha-amino acid and an aldehyde. Mioskowski *et al* (2006) presented a different approach still based on the 1,3-dipolar cycloaddition of azomethine ylides. Their approach entailed the generation of the 1,3-dipolar by double deprotonation of the corresponding trialkyl-N-oxide.[60]

2.5.4.4 Electrochemical Modification (ECM)

ECM utilises electrolysis where a thin foil bucky paper of MWCNTs is used as an electrode within an electrolytic cell. The current is passed through the electrolyte discharging the anions on the positive charged bucky-paper surface. As a result,

reactants such as oxygen or halogen atom are generated to react with the CNTs.[61] **Figure 2.6** summarizes the procedure.

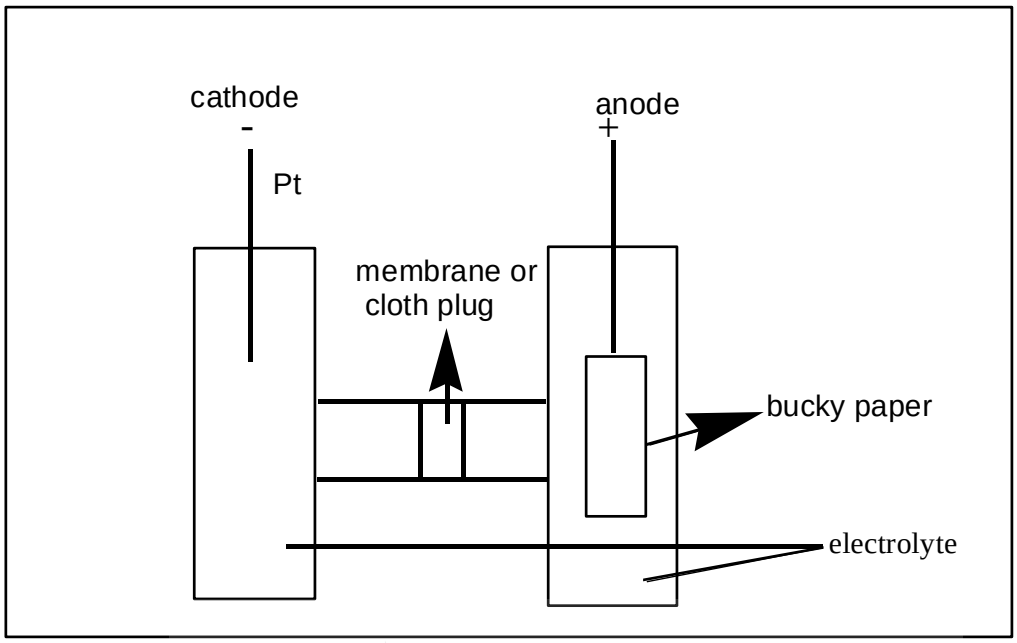

Figure 2.6: Electrolytic cell used for ECM.[61]

The ECM is unique from the other modification techniques because a desirable type of CNTs can be synthesised.[62]

2.5.4.5 Fluorination

Fluorination of CNTs or the covalent bonding of fluorine to the sidewalls of CNTs can be achieved by the use of different chemicals at different temperatures. It can be done at room temperature where a volatile fluoride, bromo trifluoride or a mixture of F_2, HF and IF_5 can be used.[63,64] Hawmi *et al* (1997) on the other hand, fluorinated CNTs using pure F_2 in a furnace.[63] However, if high temperatures are used for the fluorination, the CNT walls may be damaged yet they are also purified from amorphous carbon at these high temperatures.[63,64]

2.5.4.6 Arylation and Alkylation of CNTs

Alkylation or arylation of CNTs is also a tool used to modify CNTs. Three approaches can be used to achieve this. Firstly, several alkylithium reagents can be used to bond covalently alkyl or aryl functions to fluorinated CNTs through a displacement reaction.[65] The second approach involves the use of diazonium chemistry to attach the functions to sidewalls of CNTs.[66] And lastly, Billups reaction, which is reductive alkylation and arylation. It is utilised where lithium or sodium in liquid ammonia is used.[67]

2.5.4.7 Azide Photochemistry

Bio modification of CNTs uses azide photochemistry where an azide is added by thermolysis/photolysis to functionalized sidewalls of CNTs. This enables further biomedical application.[68]

2.6 Tributyl phosphate (TBP)

2.6.1 Background

TBP **(Figure 2.8)** is an organophosphorus compound that was first employed as an extractant in the analysis of organic acids.[69] TBP is used as an extractant because of its excellent stability and less flammability.[11] The TBP has the ability to extract lanthanides and actinides such as uranium,[69] plutonium,[69] zinc,[70] cadmium,[70] chromium,[70] titanium,[71] copper[72] and thorium.[73]

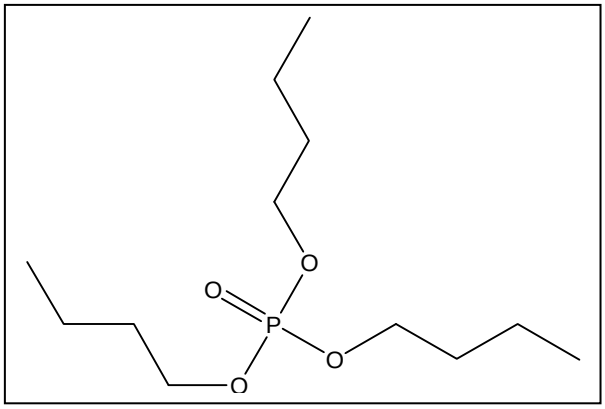

Figure 2.8: Tributyl phosphate

2.6.2 TBP complexation mechanism

During the extraction process a nitric acid-TBP complex forms, that is capable of interacting with uranium to form a complex $UO_2(NO)_3(TBP)_2$ when the anion replaces water in the co-ordination sphere of the cation.[69] Increasing the nitrate salt concentration in the solution shifts the equilibrium to the right thereby increasing the possibility of uranium extraction. Decreasing the nitric acid concentration in the solution shifts the equilibrium to the left and uranium is released from the complex $UO_2(NO)_3(TBP)_2$.[74] The extraction process is summarised by **Scheme 2.2**.

$$UO_2^{2+}{}_{(aq)} + 2NO_3^{-}{}_{(aq)} + 2TBP_{(org)} \rightleftharpoons [UO_2(NO_3)_2]\,(TBP)_{2\,(org)}$$

Scheme 2.2: Extraction of Uranyl nitrate by TBP.[75]

2.6.3 Characterisation Techniques for the Carbon nanotubes and phosphates

2.6.3.1 Scanning Electron Microscope (SEM)

The SEM is used to produce images of nano materials, where the naked eye and light microscope cannot magnify the materials because of their size. The SEM is made up of three major components namely: electron-optical column, vacuum system and electron and display system.[76] The SEM utilises a beam of electrons to illuminate the image. The electrons are generated by an electron gun accelerated at high voltage. The generated electrons are passed through an electron-optical column that is held under high vacuum. A series of deflection coils move the electron beam across the surface of the specimen and signals are produced. To give an image the signals are collected and interpreted by a detector.[77]

2.6.3.2 Transmission Electron Microscope (TEM)

The TEM operates like a slide projector. However, it differs from the latter in that it produces electrons that are focused on single, pinpoint spot on the sample. TEM differs from SEM because it uses a very thin specimen and a high acceleration voltage. The beam of electrons interacts with the specimen and travels through. The electrons that are able to travel though the specimen are projected onto the screen to produce an image. Nevertheless, some electrons fail to pass through the specimen and get absorbed forming darker parts of the image.[78]

2.6.3.3 Fourier Transform Infrared Spectroscopy (FTIR)

This absorption spectroscopy utilizes the infrared portion of the electromagnetic spectrum to examine samples. The spectroscopy produces a beam of infrared light that is split into two beams.[79] The two beams are, one at a fixed length (mirror A) and the other at a variable length (mirror B).[80] The varying distances between the two pathlengths results in destructive and constructive interferences. Thus there is variation in intensities of the interferogram.[80] The interferograms are

converted by the Fourier transformation into one spectral point on the more familiar form of the frequency domain.[80] The Fourier transform manages to give rise to a complete IR spectrum from the variation of the length between mirror A (fixed length) and mirror B (variable length).[80] An analysis is performed by placing a sample in the generated beam and determines what frequencies it absorbs. This is used for identification purposes.

2.6.3.4 Thermogravimetric Analysis (TGA)

TGA is used to determine the thermal stability and volatility of a compound as it is heated or held isothermally at a specific temperature. The TGA is operated at a temperature ranging from room temperature to 1000 °C.[81] The samples are loaded into an analyzer and an inert gas is used to purge the samples to avoid decomposition. A computer is connected to the instrument to plot weight loss against temperature. This data can be analysed to get the points of inflection.[81]

2.6.3.5 Nuclear Magnetic Resonance (NMR)

NMR identifies organic compounds and determines the structure. This technique utilises atomic nuclei and they are used because of their magnetism. The atomic nuclei are able to give information about the structure, motion and chemical reaction of the analysed sample without altering its properties.[82] The NMR tube containing the sample and a reference are introduced to the spectroscopy. Electromagnetic energy is absorbed and re-emitted by the magnetic nuclei in a magnetic field. The electromagnetic energy at a specific resonance frequency is influenced by the strength of the magnetic field and other factors. This energy is passed to the recorder.[83]

2.6.3.6 RAMAN

Raman just like FTIR spectroscopy identifies molecules by molecule vibrations. However, Raman unlike FTIR uses Raman scattering whereas FTIR uses adsorption phenomenon.[81] CNTs Raman scattering gives three prominent modes namely; G-band (graphite), D-band (disorder) and G`-band (second order Raman

scattering from D-band vibrations). CNTs also have Radial Breathing Mode (RBM) which results from a unique, prominent photon caused by isotropic radial expansion of the tubes.[84] RBM is inversely proportional to the diameter of the tubes. The ratio I_D/I_G is used to get information about the hybridisation of the carbons of the CNTs. If the value is less than one it means that the carbons are maintaining the sp^2 hybridisation whereas if it's more than one its means they are sp^3 hybridised.[84]

2.6.3.7 Energy-dispersive X-ray Spectrometry (EDX)

The EDX is coupled with the SEM. When the electrons are bombarding the specimen x-rays are emmited.[76] Analysing the energy distribution (wavelength) and intensity of the radiation gives information of the chemical composition of the specimen layer near the surface. The spectrum is plotted by x-ray intensity versus energy.[77]

2.6.3.8 Brunauer Emmet Teller

This technique is based on the adsorption of gaseous molecules from the particle surface. With this technique the surface area, pore volume and pore diameter of the particle are measured by an equation called Brunauer Emmet Teller.[85]

2.6.4 Conclusion

Radioactivity resulting from naturally occurring radionuclides and human activities generates RAW. Radioactivity is an essential part of our lives. For example, it is used in electricity generation, in hospitals for medical purposes involving use of isotopes. The nuclear facilities are faced with a challenge of storing the RAW in such a manner that the present and future generations are protected from harmful radiations. Exposure to RAW of higher radiation can result in cancer, deformities and miscarriages, to name just a few. Solvent extraction purifies the RAW and deposits liquid secondary waste that has high, long lasting radioactivity that is solidified into a matrix before deposition to underground storages. This study aims at synthesising p-MWCNTs and using them in the treatment of the RAW with the

hope of reducing the radioactivity level of RAW by adsorbing the radionuclides. CNTs are excellent adsorbents and therefore disposal of solid waste with reduced radioactivity is anticipated. The study outlined in the introduction is described in the next couple of chapters where chapter 3 describes the experimental methodology used to attain the objectives of the study.

References:

1. P.A. Baisdea and G.R. Choppin. Nuclear waste management and the nuclear fuel cycle, in Radiochemistry and Nucl. Chem, [Ed. Sandor Nagy], in Encyclopedia of life support systems (EOLSS), Developed under the Auspices of the UNESCO, Eolss Publishers, Oxford, UK, [http://www.eolss.net]. (2007). (Accessed 18 October 2008).

2. V.K. Manchanda and P.N. Pathak. Amides and diamides as a promising extractants in the back end of the nuclear fuel cycle: an overview. *Separation Purification and Technology*. **35** (2004) 85-103.

3. K. L. Nash; G. J. Lumetta; S. B. Clark and J. Friese. Significance of the nuclear fuel cycle in the 21st century, chapter 1. *ACS symposium series*. **933** (2006) 3-20.

4. J. A. Lieberman and W. G. Belter. Waste management and environmental aspects of nuclear power. *Environmental Science and Technology*. **1** (1967) 466-475.

5. P.W. Wang and R.F. Hirsch. Nuclear waste management: accomplishments of the environmental management science program, chapter 1. *ACS symposium series*. **943** (2006) 2-10.

6. W. C. Blackman Jr. Basic hazardous waste management. 3rd edt. Lewis publishers, Boca Raton, London. (2001) 352-364.

7. T.A. Todd; T.A. Batcheller; J.D. Law and R.S. Bobst. Cesium and strontium separation technologies literature review. Idaho National engineering and Environmental laboratory Bechtel BW XI, Idaho, LLC (INEEL). (2004)

8. http://www.nuclear-reprocessing-wikipedia,thefree-enclopedia. (Accessed 25 May 2009)

9. G.R. Choppin and M.K. Khankhasayev. Chemical separation Technologies and related problems of nuclear waste management: application, problems and research needs. *Environmental Security*. **53** (1999) 2-16.

10. P.W. Naik; P.S. Shami; S.K. Misra; U. Jambunathan and J.N. Mathur. Use of organophosphorus extractants impregnated on silica gel for the extraction chromatographic separation of minor actinides from high level waste solutions. *Journal of Radionalytical and Nuclear Chemistry*. **257** (2003) 327-332.

11. G.R. Choppin and A. Morgenstern. Radionuclide separations in radioactive waste disposal. *Journal of Radioanalytical and Nuclear Chemistry*. **242** (2000) 45-51.

12. H.H. Dam; H. Beijleveld; D.N. Reinhoudt and W. Verboum. In the pursuit for better actinide ligands: An efficient strategy for their discovery. *Journal of American Chemical Society*. **130** (2008) 5542-5551

13. V.G. Linnik; J.E. brown; M. dowdall; V.N. Potapov and A.N. Nosov. Patterns and inventories of radioactive contamination of island sites of the Yenisey River, Russia. *Journal of Environmental Radioactivity*. **87** (2006) 188-208.

14. D. Tasis; N. Tagmatarchis; A. Bianco and M. Prato. Chemistry of carbon Nanotubes. *Chemical Society Reviews*. **106** (2006) 1105-1136.

15. A. Hirsch and O. Vostrowsky. Functionalisation of carbon nanotubes. *Topics in Current Chemistry*. **245** (2005) 193-237.

16. A. Oki; L. Adams; V. Khabashesku; Y. Edigin; P. Biney and Z. Luo. Dispersion of aminoalkylsilyl ester or amine alkyl- phosphonic acid side wall functionalized carbon nanotubes in silica using sol-gel processing. *Materials letters*. **62** (2008) 918-922.

17. http://www.ibwc.u-strasby.fr/ict/images/SWNT_MWNT.jpg. (Accessed 17 August 2008)

18. M.S Mauter and M. Elimelech. Environmental applications of carbon-based nanomaterials. *Environmental Science and Technology*. Article in press.

19. J. Hu; C. Chen; X. Zhu and X. Wang. Removal of chromium from aqueous solution by using oxidised multiwalled carbon nanotubes. *Journal of Hazardous Material*. **162** (2009) 1542-1550.

20. C.R.T. Tarley; V. S. Santos; B.E.L Baeta; A.C. Pereira and L. T. Kubota. Simultaneous determination of zinc, cadmium and lead in environmental water samples by potentiometric stripping analysis (PSA) using multiwalled carbon nanotubes electrode. *Journal of Hazardous Materials*. **169** (2009) 256-262.

21. J.P. Xiao; Q.X. Zhou and H.H. Bai. Application of multiwalled carbon nanotubes treated by potassium permanganate for determination of trace cadmium prior to flame atomic absorption spectrometry. *Journal of Environmental Sciences*. **19** (2007) 1266-1271.

22. C. Chen; J. Hu; D. Xu; X. Tan; Y. Meg and X. Wang. Surface complexation modeling of Sr(II) and Eu (III) adsorption onto oxidized multiwall carbon nanotubes. *Journal of Colloid and Interface Science*. **322** (2008) 33-41.

23. C. Chen; J. Hu; D. Shao; J. Li and X. Wang. Adsorption behavior of multiwall carbon nanotubes/ iron oxide magnetic composites for Ni(II) and Sr(II). *Journal of Hazardous Material*. **64** (2009) 923-928.

24. S. lijima. Helical microtubules of graphitic carbon. *Nature*. **354** (1991) 56-58.

25. T.W. Ebbesen and P.M. Ajayan. Large-scale synthesis of carbon nanotubes. *Nature*. **358** (1992) 220-222.

26. T. Guo; P. Nikolaev; A.G. Rinzler; D. Tomanek; D.T. Colbert and R.E. Smalley. Self-assembly of tubular fullerenes. *Journal of Physical Chemistry*. **99** (1995) 10694-10697.

27. T. Guo; P. Nikolaev; A. Thess; D.T. Colbert and R.E. Smalley. Catalytic growth of single-walled nanotubes by laser vaporisation. *Chemical Physics Letters*. **243** (1995) 49-54.

28. A.E. Agboola; R.W. Pike; T.A. Hertwig and H.H. Lou. Conceptual design of carbon nanotubes processes. *Clean Technologies and Environmental* Policy. **9** (2007) 289-311.

29. P.L. Jr. Walker; J.F. Rakszawski and G.R. Imperial. Carbon formation from carbon monoxide-hydrogen mixtures. *Journal of Physical Chemistry*. **63** (1959) 133-140.

30. M Jose-Yacaman; M. Miki-Yoshida and L. Rendon. Catalytic growth of carbon microtubules with fullerenes structures. *Applied Physics Letters*. **62** (1993) 657-659.

31. http://en.wikipedia.org/wiki/carbon_nanotube. (Accessed 4 February 2009).

32. N. Inami; M.A. Mohamed; E. Shikoh and A. Fujiwara. Synthesis-condition dependence of carbon nanotubes growth by alcohol catalytic chemical vapor deposition method. *Science and Technology of Advanced Material*. **8** (2007) 292-295.

33. N. Ishigami; H. Ago; K. Imamoto; M. Tsuji; K. Lakoubovskii and N. Minami. Crystal plane dependent growth of aligned single-walled carbon nanotubes on sapphire. *Journal of American Chemical Society*. **130** (2008) 9918-9924.

34. M. Meyyappan. Carbon nanotubes science and applications. CRC press LLC, United states of America. (2005) 99-101.

35. M. Kumar and Y. Ando. Carbon Nanotubes from Camphor: An Environment-friendly Nanotechnology. *Journal of Physics*: conference series. **61** (2007) 643-646

36. Al. Darabont; P. Nemes-Incze; K. Kertesz; L. Tapaszto; A.A. Koos; Z. Osvath; Zs. Sarkozi; Z. Vertesy; Z.E. Hervath and L.P. Biro. Synthesis of carbon nanotubes by spray pyrolysis and their investigation by electron microscopy. *Journal of Optoelectronics and advanced Materials*. **7** (2005) 631-636.

37. S.R.C. Vivekchad; L.M. Cele; F.L. Deepak; A.R. Raju; A. Govindaraj. Carbon nanotubes by nebulised spray pyrolysis**.** *Chemical Physics Letters*. **386** (2004) 313-318.

38. L. Yuan; K. Saito; C. Pan; F.A. Williams and A.S. Gordon. Nanotubes from methane flames. *Chemical Physics Letters*. **340** (2001) 237-241.

39. H.M. Duan and J.T. Mckinnon. Nanoclusters produced in flames. *Journal of Physical Chemistry*. **98** (1994) 12815-12818.

40. L. Yuan; K. Saito; W. Hu and Z. Chen. Ethylene flame synthesis of well-aligned multi-walled carbon nanotubes. *Chemical Physics Letters*. **346** (2001) 23-28.

41. L.E. Murr; J.J. Bang; E.V. Esquivel; P.a. Guerrero and D.A. Lopez. Carbon nanotubes, nanocrystals forms and complex nanoparticles aggregates in common fuel-gas combustion sources and the ambient air. *Journal of Nanoparticles research.* **6** (2004) 241-251.

42. K. Hernadi. MTA SzFKI carbon nanotubes learning seminar. Purification of carbon nanotubes. (2005) University of Szeged.

43. L. Thin-Nga; K. Hernadi; E. Ljubovic; S. Garaj and L. Forr. Mechanical purification of single-walled carbon nanotubes bundles from catalytic particles. *Nano letters*. **2** (2002) 1349-1352.

44. T. Ndzimandze. Msc. Dissertation. Phosphorylation of multi-walled carbon nanotubes. (2007). University of Johannesburg.

45. K. Herandi; A. Siska; L. Thien-Nga; L. Forro and I. Kiricsi. Reactivity of different kinds of carbon during oxidative purification of catalytically prepared carbon nanotubes. *Solid state Ionics*. **141-142** (2001) 203-209.

46. Y. Zhang; Z. Shi; Z. Gu and S. iijima. Structure modification of single-wall carbon nanotubes. *Carbon*. **38** (2000) 2055-2059.

47. K. Hernadi; A. Fonseca; J.B. Nagy; D. Bernaerts; J. Riga and A. Lucas. Catalytic synthesis and purification of carbon nanotubes. *Synthetic Metals*. **77** (1996) 31-34.

48. H. Kuzmanyi; A. Kukovecz; F. Simon; M. Holzweber; Ch. Kramberger and T. Pitchler. Funtionalisation of carbon nanotubes. *Synthetic metals*. **141** (2004) 113-122.

49. G. Chao; Y. Z. Jin; H. Kong; R.L.D. Whitby; S.F.A. Acquah; G.Y. Chen; H. Quia; A. Hartschub; S.R.P. Silva; S. Henley; P. Fearon; H.W. Kroto and D.R.M. Walton. Polyurea-functionalised multiwalled carbon nanotubes: synthesis, morphology, and Raman spectroscopy. *Journal of Physical Chemistry* B. **109** (2005) 11925-11932.

50. Y. Sun; K. Fu; Y. Lin and W. Huang. Functionalised carbon nanotubes: properties and applications. *Accounts of Chemical Research*. **35** (2002) 1096-1104.

51. S. Pekker; J.P. Salvetat; J.M. bonard and L. Forro. Hydrogenation of carbon nanotubes and graphite in liquid ammonia. *Journal of Physical Chemistry B*. **105** (2001) 7938-7943.

52. Y. Hattori; Y. Watanabe; S. Kawasaki; F. Okoni; B.K. Pradhan; T. Kyotani; A. Tomita and H. Touhara. Carbon-alloying of the rear surface of nanotubes by direct fluorination. *Carbon*. **37** (1999) 1033-1038.

53. V. Georgakilas; K. Kordatos; M. Prato; D.M. Guldi; M. Holzinger and A. Hirsch. Organic functionalisation of carbon nanotubes. *Journal of American Chemical Society*. **124** (2002) 760-761.

54. Y. Sun; S. R. Wilson and D.I. Schuster. High dissolution and strong light emission of carbon nanotubes in aromatic amine solvents. *Journal of American Chemical Society*. **123** (2001) 5348-5349.

55. L. Zeng; W. Wang; J. Liang; Z. Wang; Y. Xia; D.Lei; X. Ren; N. Yao and B. Zhang. The change of morphology, structure and optical properties from carbon nanotubes treated by hydrogen plasma. *Materials Chemistry and Physics*. **108** (2008) 82-87.

56. Y. Wang; Z. Iqbal and S.V. Malhotra. Functionalisation of carbon nanotubes with amines and enzymes. *Chemical Physics Letters*. **402** (2005) 96-101.

57. V. Datsyuk; M. Kalyva; K. Papagelis; J. Parthenious; D. Tasis; A. Siokou; I. Kallitsis and C. Galiotis. Chemical oxidation of multiwalled carbon nanotubes. *Carbon*. **46** (2008) 833-840.

58. X. Yu; B. Lin; B. Gong; J. Lin; R. Wang and K. Wei. Effect of nitric acid treatment on carbon nanotubes (CNTs)-cordierite monoliths supported ruthenium catalyst for ammonia synthesis. *Catalysis Letters*. **124** (2008) 168-173.

59. X. Li; J. Shi; Y. Qin; Q. Wang; H. Luo; P. Zhang; Z. Guo; H. Woo and D. Park. Alkylation and arylation of single-walled carbon nanotubes by mechanochemical method. *Chemical Physics Letters*. **444** (2007) 258-262.

60. C. Menard-Moyon; N. Izard; E. Doris and C. Mioskowski. Separation of semiconducting from metallic carbon nanotubes by selective functionalisation with azomethine ylides. *Journal of American Chemical Society*. **128** (2006) 6552-6553.

61. E. Unger; A. Graham; F. Kreupl; M. Liebau and W. Hoenlein. Electrochemical functionalisation of multi-walled carbon nanotubes for solvation and purification. *Current Applied Physics*. **2** (2002) 107-111.

62. K. Balasubramanian. Seminar. Electrochemical functionalisation of carbon nanotubes and device applications. (June 28, 2006). Universitat Rovira, virgili, Tarragona, Spain.

63. A. Hamwi; H. Alvergnat; S. Bonnamy and F. Beguin. Fluorination of carbon nanotubes. *Carbon*. **35** (1997) 723-728.

64. A.V. Okotrub; N.F. Yudanov; A.L. Chuvilin; I.P. Asanov; Y.V. Shubin; L.G. Bulusheva; A.V. Guselnikov and I.S. Fyodorov. Fluorinated cage multiwall carbon nanoparticles. *Chemical Physics Letters*. **322** (2000) 231-236.

65. S. Chen; W. Shen; G. Wu; D. Chen and M. Jiang. A new approach to the functionalisation of single-walled carbon nanotubes with both alkyl and carbonyl groups. *Chemical Physics Letters*. **402** (2005) 312-317.

66. R.K. Saini; I.W. Chiang; H. Peng; R.E. Smalley; W.E. Billups; R.H. Hauge and J.L. Margrave. Covalent sidewall functionalisation of single wall carbon nanotubes. *Journal of American Chemical Society*. **125** (2003) 3617-3621.

67. J.J. Stephenson; A.K. Sadana; A.L. Higginbotham and J. M. Tour. Highly functionalised and soluble multiwalled carbon nanotubes by reductive alkylation and arylation: the Billups reaction. *Chemistry of Materials.* **18** (2006) 4658-4661.

68. W. Yang; P. Thordarson; J.J. Gooding; S.P. Ringer and F. Braet. Carbon nanotubes for biological and biomedical applications. *Nanotechnology*. **18** (2007) 1-12.

69. L.L. Burger. Uranium and plutonium extraction by organophosphorus compounds. Hanford laboratories operation, general electric company, Richland, Washington. **62** (1957) 590-593.

70. A. Mellah and D. Benachour. The solvent extraction of zinc, cadmium and chromium from phosphoric acid solutions by tri-n-butyl phosphate in kerosene diluent. *Separation and Purification Technology.* **56** (2007) 220-224.

71. S. Seyfi and M. Abdi. Extraction of titanium (IV) from acidic media by tri-n-butyl phosphate in kerosene. *Minerals Engineering*. **22** (2009) 116-118.

72. J.C Lee; T. Zhu; M.K. Jha; S.K. Kim; K.K. Yoo and J. Jeong. Solvent extraction of Cu(II) from waste etch chloride solution using tri-butyl phosphate (TBP) diluted in 1-octanol. *Separation and Purification Technology*. **62** (2008) 596-601.

73. Y. Lin; C.M. Wai; F.M. Jean and R.D. Brauer. Supercritical fluid extraction of thorium and uranium ions from solid and liquid materials with fluorinated β-Diketones and tributyl phosphate. *Environmental Science and Technology*. **28** (1994) 1190-1193.

74. Y. Lin; N.G. Smart and C.M. Wai. Supercritical fluid extraction of uranium and thorium from nitric acid solution with organophosphorus reagent. *Environmental Science and Technology*. **29** (1995) 2706-2708.

75. K. Nukada; K. Naito and U. Maeda. On the mechanism of the extraction of uranyl nitrate by tributyl phosphate II. Infrared study. **33** (1960) 894-898.

76. G. Lawes. Scanning electron microscopy and X-ray microanalysis. Published on behalf of Analytical chemistry by open learning, Thames Polytechnic, London by John Willey and sons. (1987) 1-7.

77. S.K. Chapman. Working with a scanning electron microscope. Lodgemark Press bank house, summerhill, Chislehurst dent BR7 5RD, England. (1986) 11-12.

78. G. Boon. Simultaneous determination of specimen composition and thickness using the transmission electron microscope. Technische Universiteit Eindhoven (2000) 1-3.

79. B.C. Smith. Fundamentals of Fourier transform infrared spectroscopy. C.R.C. Press. Boca Raton London, New York, Washington D.C. (1996) 15-53.

80. R.M Silverstone; F.X. Webster and D.J. Kiemle. Spectrometric identification of organic compounds. 7th edition. John wiley and sons, Inc. USA. (2005) 78.

81. A.S. Frank. Handbook of instrumental techniques of analytical chemistry. PTR Prentice-Hall, Inc A Simon and Schuster Company, upper saddle river, New Jersey (1997) 285-911.

82. P.J. Hore. Nuclear magnetic resonance. Oxford publications. New York Tokyo. (1995) 1-5.

83. http://en.wikipedia.org. (Accessed 13 April 2011)

84. M.S. Dresselhaus; g. Dresselhaus; R. Saito and A. Jorio. Physics report. **409** (2005) 47-99.

85. http://www.fei.lt/en/analytical.htm. (Accessed 1 June 2010)

CHAPTER 3

EXPERIMENTAL METHODOLOGY

3.1 Introduction

In this chapter, the experimental procedures used to attain the objectives of the project are outlined. The procedures include the following aspects: synthesis and functionalisation of the MWCNTs, synthesis of phosphorylating reagent, phosphorylation of the MWCNTs and their application in the treatment of RNW. The results are discussed in the following chapter.

3.2 Chemicals and Reagents

The chemicals used in this project were analytical grade and they were purchased from either Merck or Aldrich. The reagents and solvents used were purified by known laboratory procedures.

3.3 Characterisation of Samples

3.3.1 Instrumentation

Jeol Jsm-5600 Scanning Electron Microscope (SEM), Tecnai G^2 spirit Transmission Electron Microscope (TEM), Midac (model 4000) Fourier Transform Infrared (FTIR) spectroscopy, Energy-dispersive X-ray Spectroscopy (EDX), Raman, Thermo gravimetric analysis (TGA) Brunauer Emmet Teller (BET), UV-visible Spectrophotometer and Scanning X-ray photoelectron Spectroscopy were used for characterisation.

3.3.2 Preparation of samples for characterisation

3.3.2.1 Fourier Transform Infrared

About 2.00 mg of MWCNT samples and excess KBr were mixed thoroughly using a pestle and mortar. The mixture was fed into a mechanical press to form a pellet. After 5 minutes the pellet was removed from the press machine and put into a pellet holder. The sample or pellet holder with the sample was then introduced to the MIDAC FTIR (model 4000) spectrometer. The number of scans used was 16 at a resolution of 4 cm^{-1}. A background was taken before the sample was scanned.

3.3.2.2 Scanning Electron Microscope

A carbon tape was fixed on a slide. A sample was mounted on to the carbon tape. The sample was gold coated. The coated sample was then put into a Jeol Jsm-5600 SEM. Proper focusing was done resulting in the formation of an image.

3.3.2.3 Energy-dispersive X-ray Spectrometry

The sample was prepared just like for SEM, the difference is that the samples were carbon coated. The sample was placed into the SEM and proper configurations and focusing were done. Software for the easy EDX was then used to produce the EDX results.

3.3.2.4 Transmission Electron Microscope

Samples were sonicated in methanol for 10 minutes. A pipette was used to introduce sample to a grid. The grid was then put inside a tip of the sample holder. The tip was introduced into the TEM. Correct adjustment and focusing were done to enable production of an image.

3.3.2.5 Raman

Jobin-Yvon T64000 Raman Spectrometer was used to run the MWCNTs samples. The instrument was operated at a single spectrograph mode with 600 lines per millimetre grating. An excitation source of a 514.5 nanometre line from an argon ion laser was used. To focus laser onto the sample an objective lens of 20X magnification of an olympus microscope was used. To prevent local heating a 1.2 mV laser power was kept with the sample. Scattered light was collected in a backscattering configuration. A nitrogen cooled CCD detected the scattered light.

3.3.2.6 Thermo Gravimetric Analysis

A Perkin Elmer Pyris 1 Thermal Gravimetric analyzer was utilised to determine the stability of the MWCNTs samples. Before the start of the analysis, N_2 gas was run through the instrument. About 0.010 g of the MWCNTs samples were introduced to the TGA. The samples were ramped from ambient temperature to 900 °C at a heating rate of 10 degrees per minute under oxygen. The oxygen flow rate used was 20 degrees per minute. Weight loss with increase in temperature was automatically recorded.

3.3.2.7 NMR

Sample preparation for NMR is dependent on the type of analysis to be done. For example between 20-50 mg for ^{13}C and 5-25 mg for ^{1}H. The sample is dissolved in a deuterated solvent and the height of the mixture should be 5 cm in the NMR tube. The NMR tube is introduced to the NMR where appropriate configurations are done and the resulting spectrum is printed for analysis.

3.3.2.8 Brunauer Emmet Teller

At least about 0.2 g of samples were degassed in N_2 at 120 °C for 4 hours prior to analysis using a micromeritics Flow Prep 060, sample degas system. The surface areas and pore size distributions were then obtained at 196 °C. The pore size distribution with specific surface areas of the samples, were determined via N_2

adsorption/desorption according to the BET method using a Micromeritics Tristar, surface area and porosity analyzer. In order to confirm the accuracy of the results, the analysis was repeated at least twice for all samples and the measurements were in good agreement.

3.3.2.9 UV-visible Spectrophotometer

A Cary 100 UV-Visible instrument was used to determine the ratio of a tracer distribution between a liquid and solid phase. A programme of 6.01 was used for the analysis. The spectroscopy was switched on an hour before the analysis to allow sufficient heating up time. The wavelength used for the analysis was 450.0 nm and an SBW of 1.5 nm. Blanks and standards were run before the absorbances of the samples were recorded.

3.3.2.10 Scanning X-ray photoelectron Spectroscopy (SXPS)

A small amount of MWCNT samples were analysed with a physical electron Quantum2000 SXPS to determine their surface composition. The X-rays used were Al K∞ (1486 eV) with X-ray power of 20 W. The beam diameter used was 100 µm. The wide and narrow pass energy used were 117.4 and 29.35 eV respectively.

3.4 Experimental Procedure

Scheme 3.1 summarises the experimental procedure used to attain the objectives of the study.

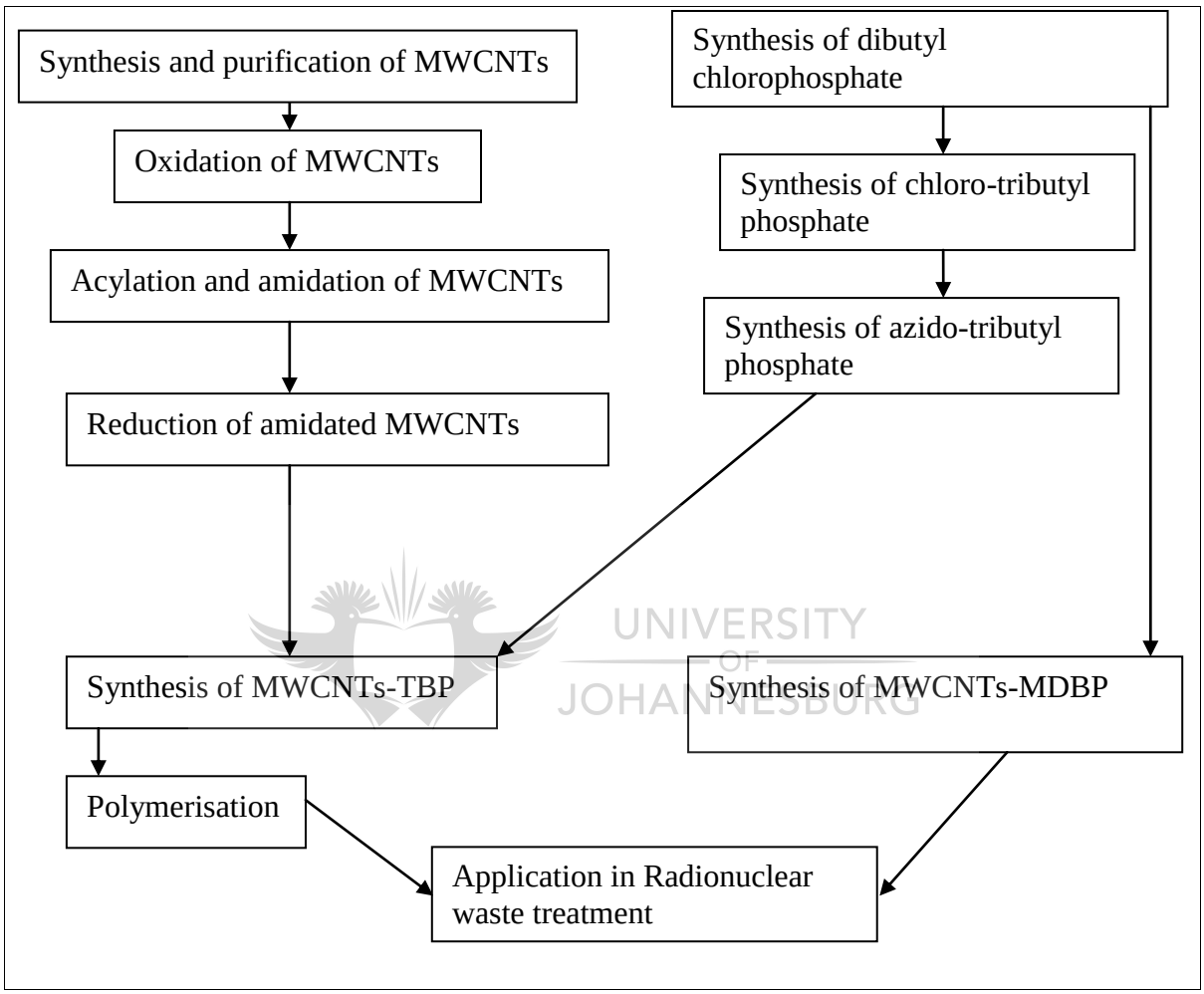

Scheme 3.1: The summary of the methodology.

3.4.1 MWCNTs synthesis

MWCNTs were synthesised using the nebulised spray pyrolysis (NSP) technique. As per the procedure reported by Vivekchad *et al* (2004), 2 g ferrocene (catalyst) was dissolved in 50 mL toluene (carbon source) to make a solution. A syringe was used to feed the solution to an atomization chamber that was then connected to the rest of the set up as shown in **Figure 3.1**. Electrical power was applied and the nebulizer produced a spray which was carried by argon flowing at a rate of

500 sccm (standard cubic centimetres per minute) to a quartz tube housed by a furnace which was heated at 900 °C. After 45 minutes the furnace was turned off and the gas flow rate was decreased to 80 sccm. This was left overnight to allow the furnace to cool down after which the gas flow was stopped and quartz tube taken out of the furnace. The MWCNTs deposited in the tube were scraped out by means of a wooden stick.[1] The yield obtained was 0.835 g.

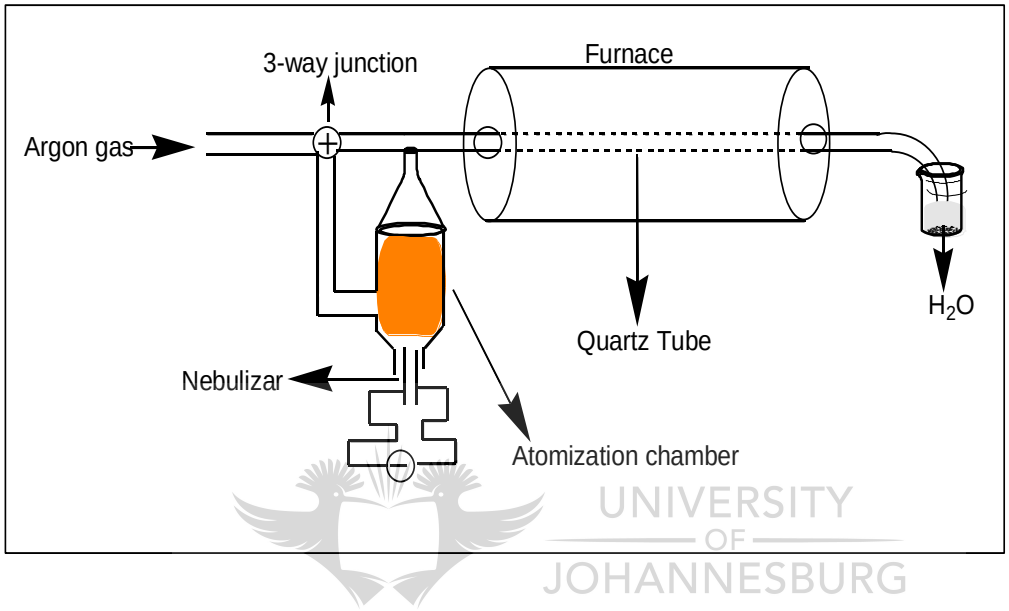

Figure 3.1: The experimental set up for MWCNTs synthesis by NSP

3.4.2 Purification of the MWCNTs

The synthesized MWCNTs were burnt in an oven at 350 °C for 30 minutes to remove amorphous carbon. To remove the fullerenes, a soxhlet extractor was utilized to reflux the MWCNTs for 24 hours. The MWCNTs were fed into an extraction thimble which was introduced into the extractor as illustrated in **Figure 3.2**. The CNTs were then dried in a vacuum oven at 50 °C for 24 hours.

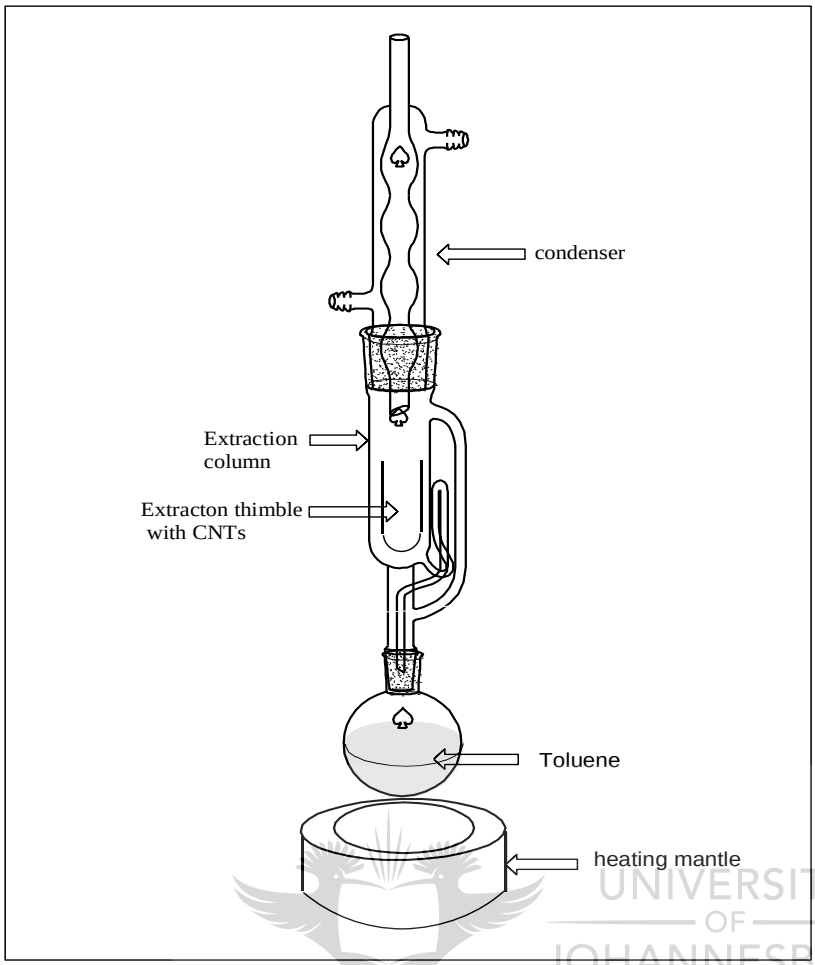

Figure 3.2: The soxhlet extractor

3.4.3 Functionalisation of the MWCNTs

3.4.3.1 Oxidation of MWCNTs

Pristine MWCNTs (2.0 g), 98 % H_2SO_4 (60 mL) and 55 % HNO_3 (30 mL) were added to a one-necked round bottom flask equipped with a condenser. The mixture was stirred at 90 °C for an hour. **Scheme 3.2** illustrates the reaction pathway for the oxidation of the MWCNTs. After cooling to room temperature, the mixture was diluted with 50 mL of distilled water and filtered through a 0.45 µm PTFE membrane as outlined by Chao *et al.* (2005).[2] The oxidised MWCNTs were dried in a vacuum oven at 50 °C for 24 hours. **Yield:** 1.88 g. 94 % yield (mass: mass).

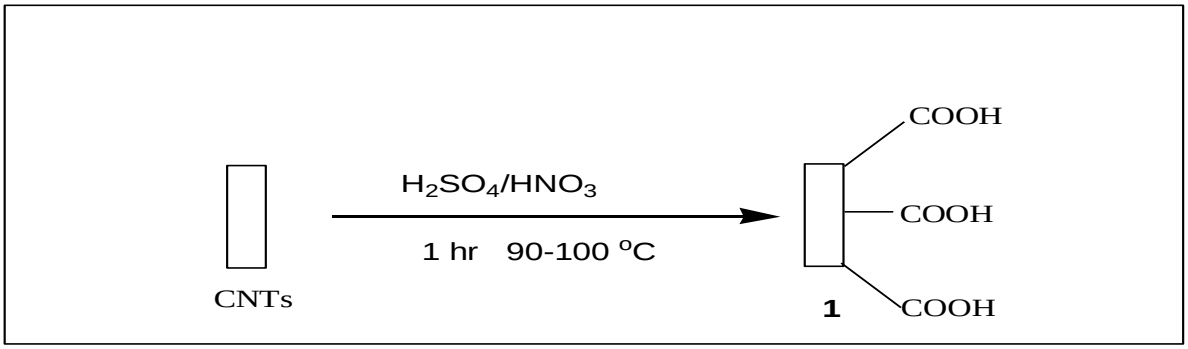

Scheme 3.2: Reaction pathway for oxidation of MWCNTs.

3.4.3.2 Acylation and amidation of MWCNTs

Oxidised MWCNTs (0.52 g) were sonicated in 100 mL of dimethyl formaldehyde (DMF) at room temperature for 30 minutes. The mixture was fed into a 3-necked round bottom flask. To the mixture, oxalyl chloride (15 mL, 0.174 mol)) was added dropwise at 0 °C and the mixture was stirred for 2 hours. The temperature was raised to room temperature and stirring continued for another 2 hours. The temperature was further raised to 70 °C and mixture was stirred for 18 hours to remove excess oxalyl chloride according to Wang *et al* (2005). [3] The first part of **Scheme 3.3** summarises the acylation reaction.

Didecylamine (1.2 g, 0.00403 mol) was sonicated in DMF (100 mL). It was added to the mixture of acyl-chlorinated MWCNTs and the temperature was raised to 110 °C, stirring continued for five days. Afterwards this reaction was cooled to room temperature and filtered using a 0.45 µm PTFE membrane. DMF and ethanol were used for washing as per procedure reported by Wang *et al* (2005).[3] The product was dried in a vacuum oven at 50 °C for 48 hours. The amidation reaction is shown in last step of **Scheme 3.3**.

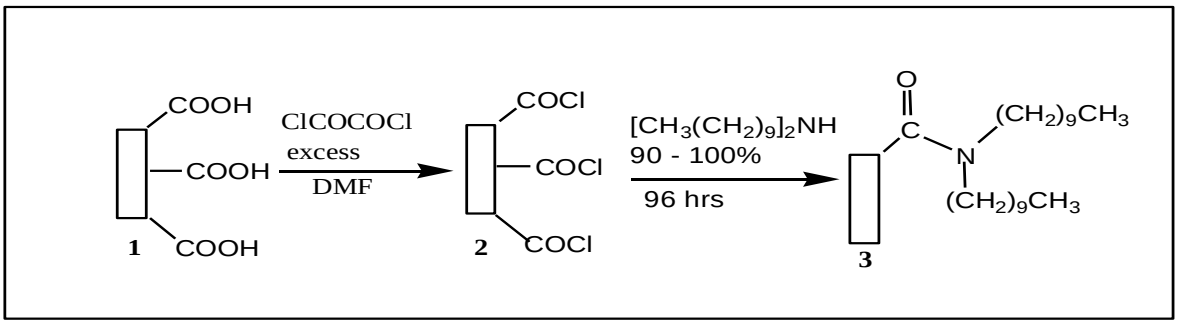

Scheme 3.3: The reaction pathway for acylation and amidation of MWCNTs

3.4.3.3 Reduction of Amidated MWCNTs

Amidated MWCNTs were sonicated in 40 mL tetrahydrofuran (THF) for 15 minutes. The mixture was fed into a 3-necked round bottom flask. Lithium aluminium hydride (10 mL, 0.235 mol) dissolved in anhydrous THF (20 mL) was added dropwise to the flask. The reaction mixture was stirred under reflux in an inert atmosphere for 48 hours. It was cooled to room temperature and 2 M HCl (40 mL) was added to the reaction mixture to separate phases. The phases were allowed to separate and the clear liquid was decanted. The black solid was washed with distilled water and dried in a vacuum oven as per the procedure by Luqu *et al* (2003).[4] **Scheme 3.4** summarises the reaction. **Yield**: 0.445 g, 86 % yield (mass: mass).

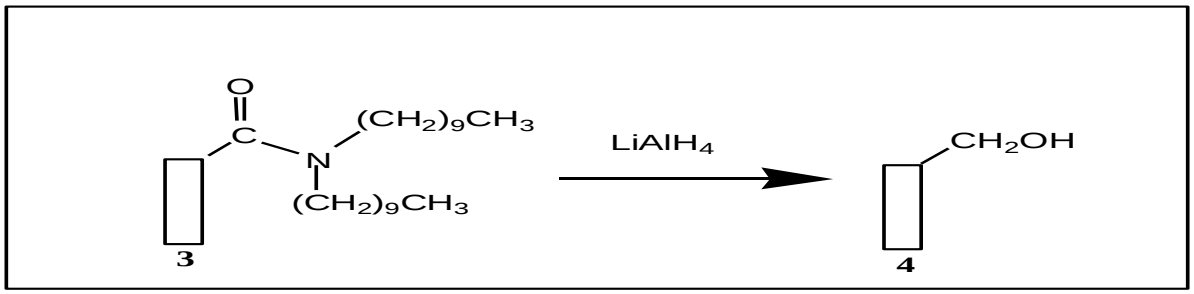

Scheme 3.4: The reduction of amidated MWCNTs.

3.4.4 Synthesis of phosphorylating reagents and Phosphorylation of MWCNTs

3.4.4.1 Synthesis of Dibutyl chlorophosphate

The synthesis was done according to **Scheme 3.5**. Into a 500 mL 3-necked round bottom flask, triethylamine (12 mL, 0.394 mol), phosphorus trichloride (12 mL, 0.131 mol) dissolved in toluene (48 mL) were added. Into the flask butanol (12 mL, 0.394 mol) dissolved in toluene (48 mL) was added dropwise. The reaction mixture was stirred at 0 °C for 20 minutes. Temperature was raised to room temperature and reaction was left over night. Sulfuryl chloride (12 mL, 0.131 mol) dissolved in toluene (24 mL) was introduced to the flask dropwise with continuous stirring at 0 °C for 35 minutes. **Figure 3.3** shows the set-up which was used for this reaction. Distillation at reduced pressure was utilized for purification purposes.[5] A colourless liquid was obtained (16.34 g, 54 % yield, 67 °C at 1.05 torr). **^{1}H NMR ($CDCl_3$)**: δ 3.459 (t, 2H, $C\underline{H}_2$-O $^{3}J_{H-H}$ = 6.9 Hz), δ 1.685 (quintet, 2H, $C\underline{H}_2$-CH_2, $^{3}J_{P-H}$ = 7.5 Hz), δ 1.414 (sextet, 2H, $C\underline{H}_2$-CH_3, $^{3}J_{H-H}$ = 7.5 Hz), δ 0.876 (t, 2H, CH_2-$C\underline{H}_3$, $^{3}J_{H-H}$ = 7.2 Hz. **^{31}P NMR ($CDCl_3$)**: δ 5.009 ppm. **FTIR**: P=O (1253.173 cm^{-1}), P-Cl (544.073 cm^{-1}), CH_3 (2990.274 cm^{-1}), CH_2 (2825.895 cm^{-1}).

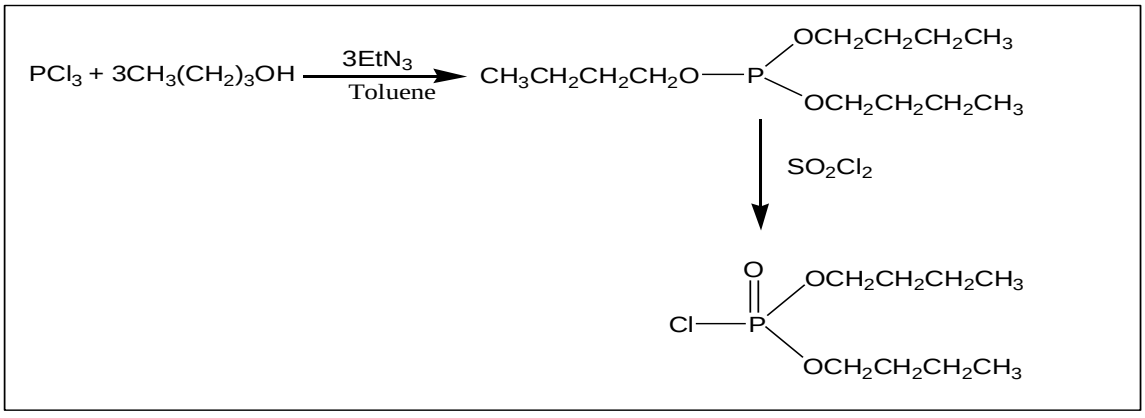

Scheme 3.5: Reaction pathway for dibutyl chlorophosphate synthesis.

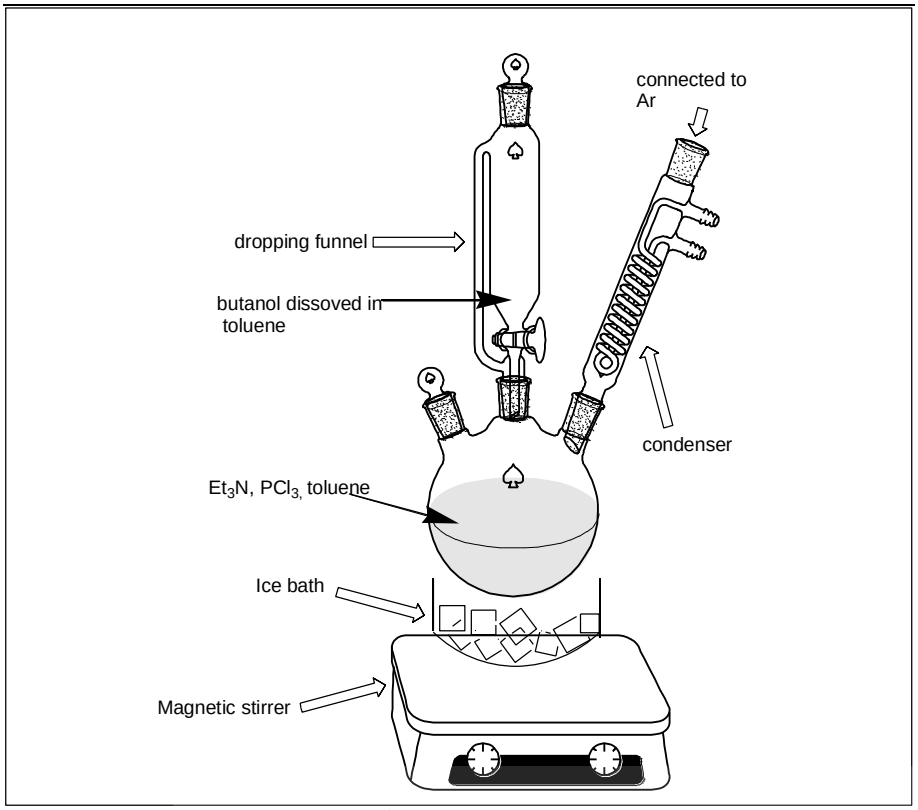

Figure 3.3: The set up used for synthesis of Dibutyl chlorophosphate

3.4.4.2 Synthesis of multiwalled carbon nanotube methylene Dibutylphosphate (MWCNTs-MDBP)

MWCNT-CH_2OH (0.040 g) and triethylamine (7 mL, 0.050 mol) were introduced into a 3-necked round bottom flask. Dibutyl chlorophosphate (7 mL, 0.0450 mol) was added dropwise to the flask. The reaction was stirred at room temperature for 24 hours. **Scheme 3.6** summarises the reaction. The product was filtered through a 0.45 µm pore size of PTFE membrane. The multiwalled carbon nanotubes-methylene dibutyl phosphate (MWCNT-MDBP) was dried in a vacuum oven at 50 °C for 24 hours. **Yield**: 0.326 g.

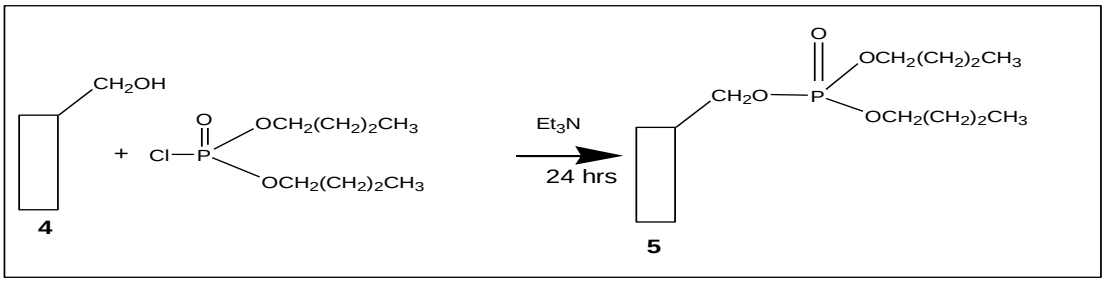

Scheme 3.6: Reaction pathway for MWCNTs-MDBP synthesis.

3.4.4.3 Chlorotributyl phosphate (Cl-TBP) synthesis

In a 3-necked round bottom flask, sodium hydride (0.70 g, 0.050 mol) was suspended in THF (33 mL). Into this mixture chlorobutanol (5.43 g, 0.050 mol) was introduced dropwise with continuous stirring under reflux at 55 °C. Dibutyl chlorophosphate (7 mL, 0.05 mol) was added dropwise to the mixture and the reaction was left under vigorous stirring for five days. The solvent was removed using a rotary evaporator. The reaction mixture was partitioned between water (30 mL) and ethyl acetate (60 mL). The organic phase was dried with anhydrous magnesium sulphate, filtered then concentrated in a rotary evaporator. Column chromatography was used to purify the product. This methodology was taken and modified from the procedure of McDougal *et al* (1986)[6] and is summarised in **Scheme 3.7**. **^{1}H NMR ($CDCl_3$)**: δ 4.036(m, 2H,C<u>H</u>$_2$-Cl, $^{3}J_{H-H}$ = 7.2 Hz), δ 3.469 (m, 2H, C<u>H</u>$_2$-O $^{3}J_{H-H}$ = 2.7 Hz), δ 1.952 (quintet, 2H, C<u>H</u>$_2$-CH_2 $^{3}J_{H-H}$ = 12 Hz), δ 1.763 (quintet, 2H, CH_2-C<u>H</u>$_2$, $^{3}J_{H-H}$ = 2.4 Hz), δ 1.611 (s, 2H, C<u>H</u>$_2$-CH_3, $^{3}J_{H-H}$ = 6 Hz), δ 1.189 (t, 2H, CH_2-C<u>H</u>$_3$, $^{3}J_{H-H}$ = 6.9 Hz). **^{31}P NMR ($CDCl_3$)**: δ -0.952 ppm. **FTIR**: P=O (1118.059 cm^{-1}), CH_3 (2966.792 cm^{-1}), CH_2 (2863.394 cm^{-1})

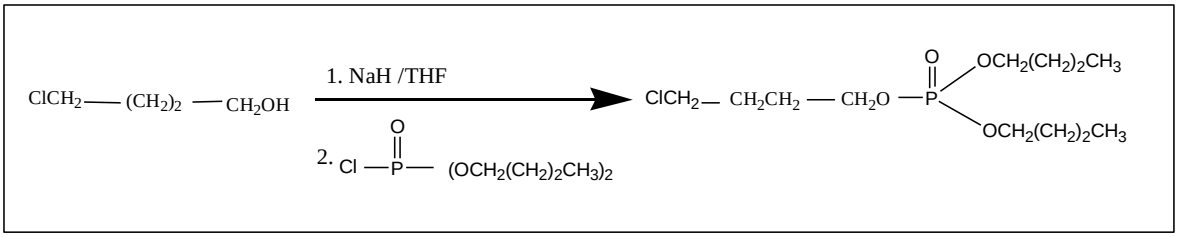

Scheme 3.7: Reaction pathway for Cl-TBP

3.4.4.4 Synthesis of azido-tributyl phosphate (azido-TBP)

Azido-TBP was synthesized as in **Scheme 3.8**. Cl-TBP (4 mL, 0.0152 mol) was added to an aqueous solution of sodium azide (4.5 g, 0.0692 mol) and tetrabutylammonium bromide (0.18 g, 0.0558 mol). The mixture was stirred under reflux at 80 °C for 24 hours then at room temperature for 15 hours. The reaction mixture was extracted with diethyl ether (3x30 mL). The organic phase was dried with anhydrous magnesium sulphate, filtered and concentrated in a rotary evaporator as per procedure outlined by J. Zhu *et al* (2007).[7] **^{1}H NMR ($CDCl_3$)**: δ 4.040 (m, 2H,C<u>H</u>$_2$-N_3, $^{3}J_{H-H}$ = 6 Hz), δ 3.639 (quintet, 2H, C<u>H</u>$_2$-CH_2 $^{3}J_{H-H}$ = 6.3 Hz), δ 3.293 (quintet, 2H, CH_2-C<u>H</u>$_2$ $^{3}J_{H-H}$ = 6.3 Hz), δ 1.727 (m, 2H, O-C<u>H</u>$_2$, = 2.7 Hz), δ 1.206 (t, 2H, CH_2-C<u>H</u>$_3$, $^{3}J_{H-H}$ = 7.2 Hz. **^{31}P NMR ($CDCl_3$)**: δ 0.833 ppm. **FTIR**: P=O (1212.457 cm^{-1}), CH_3 (2940.360 cm^{-1}), CH_2 (2863.394 cm^{-1}), N_3 (2100.733 cm^{-1}).

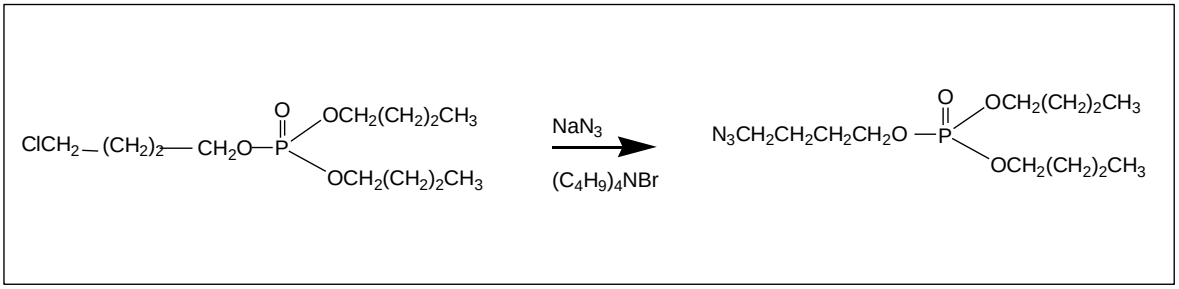

Scheme 3.8: Reaction pathway for azido-TBP.

3.4.4.5 Synthesis of multiwalled carbon nanotubes-tributyl phosphate (MWCNTs-TBP)

Into a 50 mL 2-necked round bottom flask under argon, MWCNTs-CH_2OH (0.531 g) and azido-TBP (5 mL, 0.0140 mol) were refluxed at 160 °C for 24 hours. Diethyl ether was used to wash the product. A vacuum oven at 30 °C was employed to dry the MWCNTs-TBP and they were dried for 24 hours. The reaction was done according to **Scheme 3.9.** **Yield**: 0.9424 g. **Raman spectroscopy**: D band (1354.176 cm^{-1}), G band (1581.408 cm^{-1}), I_D/I_G = 0.7. **FTIR**: C=C (1635.051 cm^{-1}), P=O (1144.491 cm^{-1}). **TGA**: 180 °C.

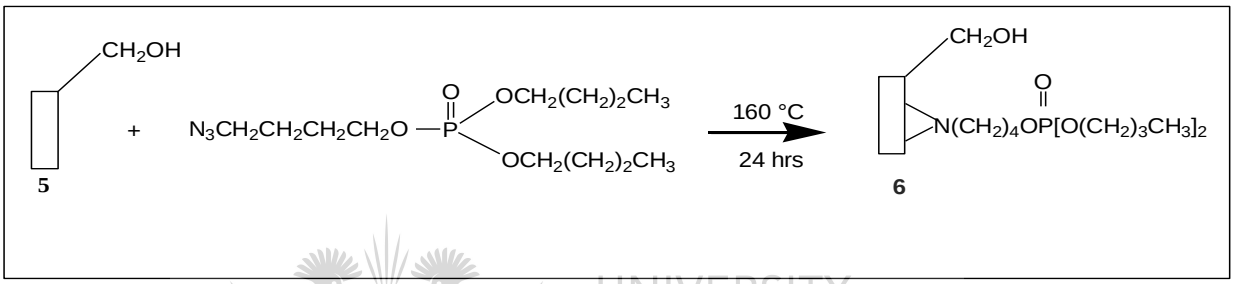

Scheme 3.9: Reaction pathway for synthesis of MWCNTs-TBP.

3.4.4.6 Synthesis of MWCNTs-TBP polymer

MWCNTs-TBP (0.900 g) were suspended in DMF (19 mL) for 15 minutes. The mixture was fed into a 50 mL 2-necked round bottom flask under an inert atmosphere. Toluene-2,4-diisocyanate (TDI), (19mL) was introduced dropwise to the mixture. The reaction was stirred at 70 °C for 24 hours. Acetone was used to wash the polymer as outlined by K.L. Salipira *et al* (2008).[8] **Scheme 3.10** shows the reaction pathway for the reaction. The polymer was dried in a vacuum oven at 30 °C for 24 hours. **Yield**: 21 g. **Raman spectroscopy:** D band (1358.063 cm^{-1}), G band (1583.296 cm^{-1}), I_D/I_G =.0.8. **FTIR**: C=C (1661.484 cm^{-1}), P=O (1144.491 cm^{-1}). **TGA**: 45 °C.

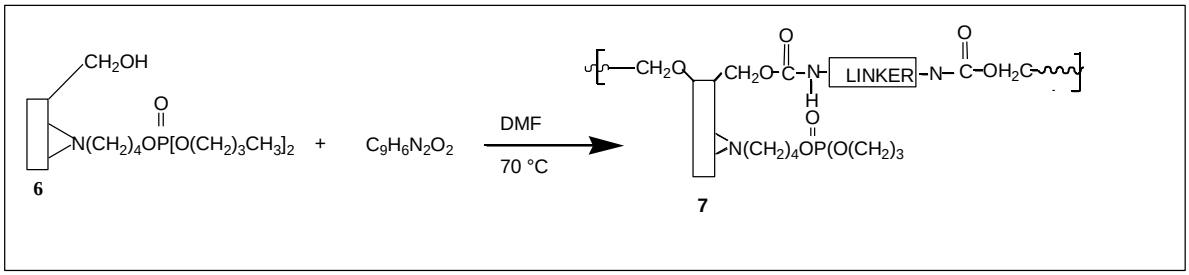

Scheme 3.10: Reaction pathway for polymerisation of MWCNTs-TBP.

3.4.5 Extraction of Uranium using pristine and functionalised MWCNTs

3.4.5.1 Procedure for determination of distribution co-efficient (Kd) values

The following method was utilised for the extraction of Uranium using pristine MWCNTs, MWCNTs-COOH, MWCNTs-MDBP and MWCNTs-TBP polymer. MWCNTs (0.04 g) and 5 mL of the pH adjusted tracer solution were introduced into a centrifuge tubes. The centrifuge tubes were immediately capped, shaken and placed in a jacket and rotated end over end at 40 r/min for 24 hours. After 24 hours the rotation was stopped and the contents of the tubes were centrifuged and the solid and liquid phase separated using a 0.45 micron syringe filter.[9]

The ratio of tracer distribution between the liquid phase and solid phase was determined by UV spectroscopy. The values of the distribution ratio ($\mathbf{K_d}$) were calculated from the following relationship:[9]

$$\mathbf{K_d} = (V/M)\,((C_o - C_i)/C_i)$$

V: volume of the solution (mL)

M: mass of MWCNTs (g)

$\mathbf{C_o}$: Initial concentration

$\mathbf{C_i}$: concentration at time i

3.4.5.2 Determination of the ratio of tracer distribution between the liquid phase and different MWCNTs samples by UV spectroscopy.

The separated liquid phases (1 mL) of each of the following samples were added into 25 mL volumetric flasks; pristine-MWCNTs, MWCNTs-COOH, MWCNTs-MDBP, MWCNTs-TBP polymer, Na_2CO_3 stock solution and HNO_3 stock solution. To each flask 3 mL of 2 M Na_2CO_3 and 30 % 1 mL of H_2O_2 were added. Water was added to the mark for each flask and the contents were mixed. A reagent blank was prepared by diluting 3 mL of 2 M Na_2CO_3 and one mL 30 % H_2O_2 to 25 mL with water. A Carey spectrophotometer was used to measure the absorbance for the standards. The spectrophotometer was switched on an hour before measurements were done to allow sufficient warm up time. The wavelength was changed to 450 nm. The 21 cm cuvettes were filled with blank solution and placed in each of the reference. Cover was closed. Absorbance value was changed to zero. The cuvette placed in sample beam was emptied and filled with one of the standard solutions. The absorbance value was recorded and procedure was repeated for all the samples. The MWCNTs samples were analysed both in acidic and basic medium.[10,11]

References:

1. S.R.C. Vivekchad; L.M Cele; F.L. Deepack; A.R. Raju and A. Govindaraj. Carbon nanotubes by nebulised spray pyrolysis. *Chemical Physics Letters*. **386** (2004) 313-318.

2. G. Chao; Y.Z Jin; H Kong; R.L.D Whitby; Acquah; G.Y Chen; H Qian; A Hartschub; S.R.P Silva; S Henley; P Fearon; H.W Kroto and D.R.M Walton. Polyurea-functionalised multiwalled carbon nanotubes: Synthesis, morphology and Raman spectroscopy. *Journal of Physical Chemistry B.* **109** (2005) 11925-11932.

3. Y. Wang; Z. Iqbal and S.V. Malhotra. Functionalisation of mutiwalled carbon nanotubes with amines and enzymes. *Chemical Physics Letters.* **402** (2005) 96-101.

4. L. Liu; Qin Y; Z. Guo and D. Zhu**.** Reduction of solubilised multiwalled carbon nanotubes. *Carbon*. **41** (2003) 331-335.

5. K. Sasse . Phosphorus derivatives. *Journal of chemical Society*. (1964) 288-290

6. P.G. McDougal; J.G. Rico; Y. Oh and B.D. Condon. A convenient procedure for the monosilylation of symmetric 1,*n*-diols. *Journal of Organic Chemistry*. **51** (1986) 3388-3390.

7. J. Zhu; X. Zhu; E.T. Kang and K.G. Neoh. Design and synthesis of star polymer with hetero-arms by the combination of controlled radical polymerisation and click chemistry. *Polymer*. **48** (2007) 6992-6999.

8 . K.L. Salipira; R.W. Krause; B.B. Mamba; T.J. Malefetse; L.M. Cele and S.H. Durbach. Cyclodextrin polyurethanes polymerized with multiwalled carbon nanotubes: synthesis and characterization. *Materials Chemistry and Physics*. **111** (2008) 218-224.

9. WCMH Meyer. Training document for the radiochemistry tracer laboratory (037)". Necsa. (2004)

10. C.J. Rodden. Analytical chemistry of the Manhattan project. 1st edition. McGraw-Hill. **1** (1950) 82-94.

11. D.J. Huyser; T.L. Sandrock; J.M. Schaekers and G.J. Van dyk. *S.A. Tydskrif vir chemie*. **39** (1986) 119

CHAPTER 4

RESULTS AND DISCUSSIONS

4.1 Introduction

This chapter discusses the results attained from the synthesis and functionalisation of the MWCNTs and their application in treatment of radioactive waste.

4.2 Scanning Electron Microscope

Figure 4.1 shows the images of MWCNTs in different stages of their functionalisation. **Fig. 4.1 (a-f)** depicts the changes in the morphology of the MWCNTs. The pristine MWCNTs illustrated in **Fig. 4.1 (a)**, are long, aligned and tubular in shape. Dispersed on top of the MWCNTs are whitish lumps, which can be attributed to traces of remains of amorphous carbon. Oxidation of the MWCNTs introduces carboxylic function and further removes the amorphous carbon. The oxidation process caused loss of alignment of the MWCNTs that is proven by **Fig. 4.1 (b)** which depicts MWCNTs resembling a blanket. Datsyuk *et al* (2008) agrees that acid treatment causes etching of the graphitic surface causing disorder and loss of alignment.[1] **Fig. 4.1 (c)**, MWCNTs-CH_2OH shows size reduction and the MWCNTs appear as a pile of stacks. Wang *et al* (2005) observed that MWCNTs-CH_2OH image appear partial blur due to reduction of contrast and resolution. This is because the CH_2OH reduces the electrical conductivity of the MWCNTs.[2] The tubes are shorter and appear in distinct strips because of the attachment of the hydroxyl functions at the ends of the tubes. Tan *et al* (2008) agrees that CNTs are prone to attachment by the functional groups at the cape and defective sides.[3] The MWCNTs-MDBP illustrated by **Fig. 4.1 (d)** show formation of clusters from the surface of the tubes. The attachment of the phosphorylating compound could have resulted in the clusters. **Fig. 4.1 (e)** which illustrates MWCNTs-TBP corresponds with **Fig. 4.1 (d)**, in the sense that it

appears as clusters. These clusters can be attributed to attachment of the tributyl phosphate. The MWCNTs-TBP polymer depicted in **Fig. 4.1 (f)** shows CNTs adhered to each other, which resulted because of polymerisation.

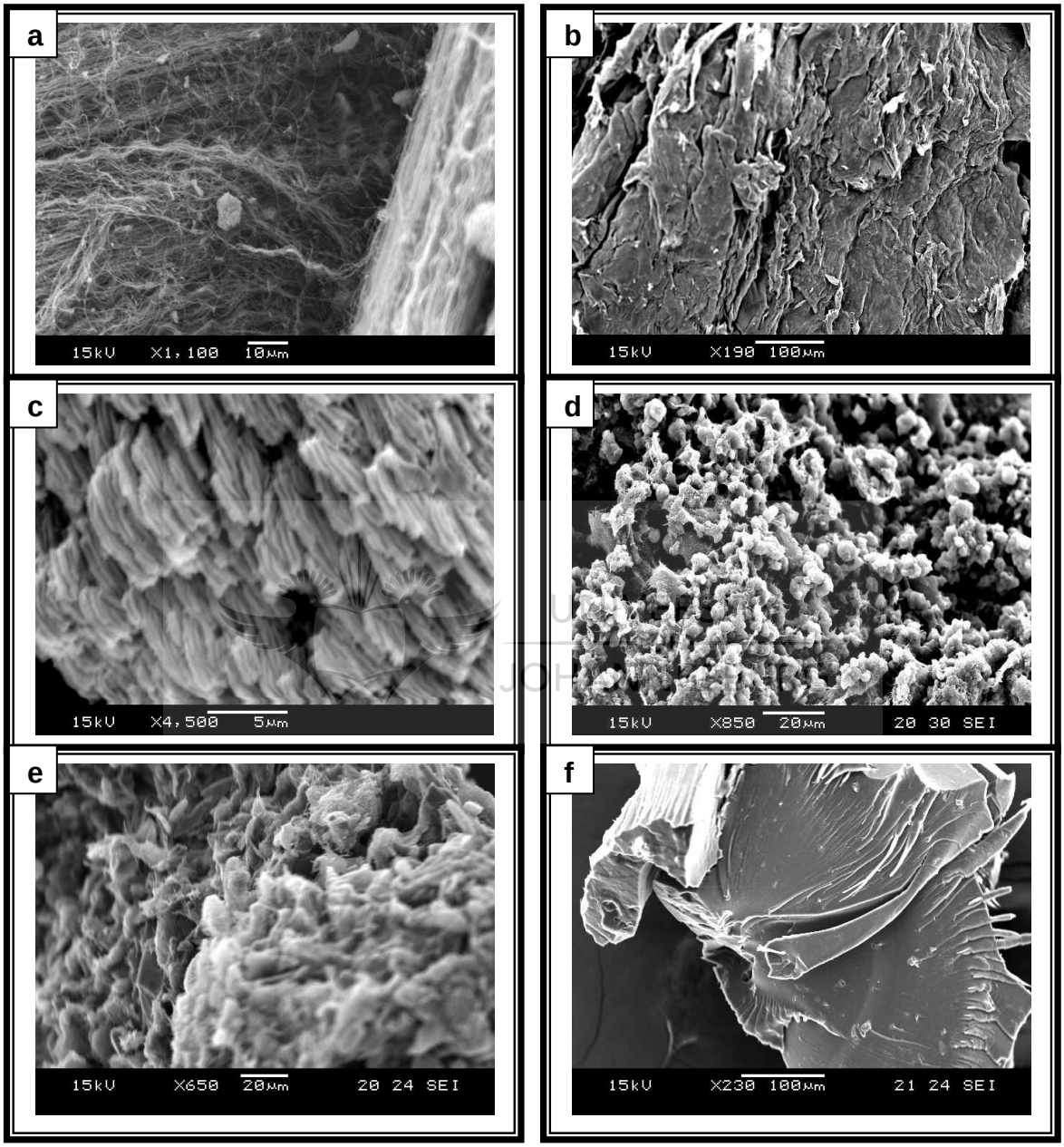

Figure 4.1: SEM images a) Pristine MWCNTs b) MWCNTs-COOH c) MWCNTs-CH_2OH d) MWCNTs-MDBP e) MWCNTs-TBP and f) MWCNTs-TBP polymer.

4.3 Transmission Electron Microscope

Figure 4.2 illustrates TEM images for pristine MWCNTs, MWCNTs-COOH, MWCNTs-CH_2OH, MWCNTs-MDBP, MWCNTs-TBP and MWCNTs-TBP polymer respectively. The pristine MWCNTs are long, curved and entangled as observed by Peng *et al* (2009).[5] Oxidation of the MWCNTs shortens and opens the ends of the tubes. Some studies have proven that open-ended CNTs have greater absorption potential than closed ends CNTs.[4] The etching of the walls observed by Tan *et al* (2008) is confirmed by the surface of MWCNTs-COOH that appears rough.[3] During the acylation, amidation and reduction processes to introduce the hydroxyl functions more wall damage to the tubes was done as shown by **Fig. 4.2 (c)**. **Fig. 4.2 (d)** which shows MWCNTs-MDBP corresponds with **Fig. 4.1 (d)**. Clusters are shown on the surface of the tubes and are attributed to the phosphorylating compound MDBP. **Fig. 4.2 (e)** and **(f)** shows CNTs entangled to each other. There is a substance situated between the entangled MWCNTs-TBP which can be attributed to TBP. **Fig. 4.2 (f)** shows a foreign black substance on the surface of the tube which can also be ascribed to the TBP.

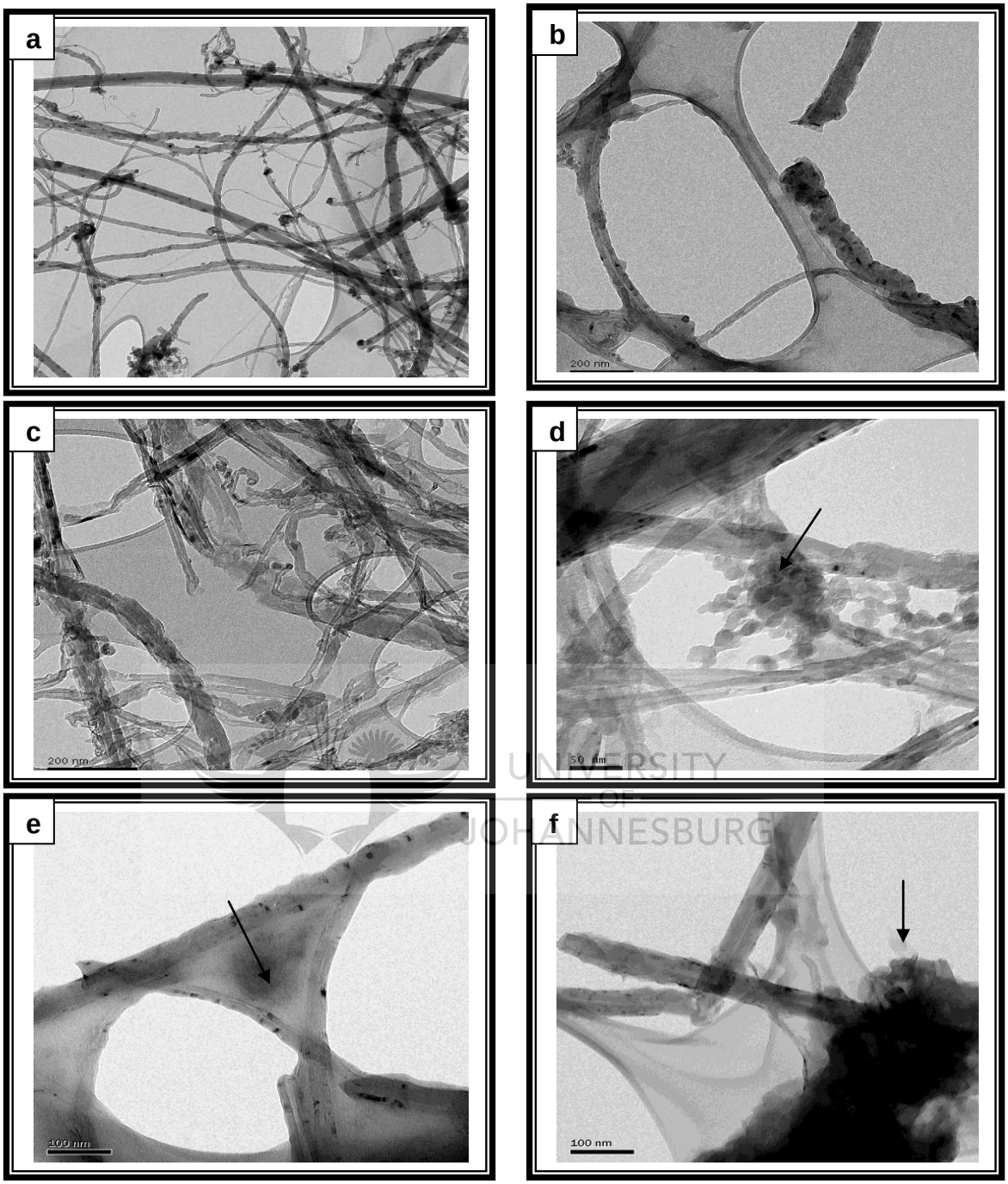

Figure 4.2: TEM images a) Pristine MWCNTs b) MWCNTs-COOH c) MWCNTs-CH_2OH d) MWCNTs-MDBP e) MWCNTs-TBP and f) MWCNTs-TBP polymer.

4.4 Fourier Transform Infrared Spectroscopy

The illustrations in **Figure 4.3** show FTIR spectra for MWCNTs at the different stages of their functionalisation. The spectrum for pristine MWCNTs **Fig. 4.3 (a)** shows MWCNTs characteristic peak at 1635.051 cm^{-1}, which is attributed to the C=C stretch. This peak is prominent in all the FTIR spectra. However, after the oxidation process additional peaks are observed as proven by **Fig. 4.3 (b).** A C=O stretch at 1726.011 cm^{-1} and O-H at 3433.913 cm^{-1} prove the incorporation of the carboxylic functions to the MWCNTs. Peng *et al* (2009) observed the C=O and O-H peaks at 1710 and 3500 cm^{-1} respectively for oxidised MWCNTs[5], which is almost the same as what we attained. **Fig. 4.3 (c)** shows additional peaks which confirms the removal of the C=O and inclusion of the C-H and OH at 2922.257 and 1060.862 cm^{-1} respectively. The MWCNTs-MDBP **Fig. 4.3 (d)** proves successful inclusion of the MDBP to the MWCNTs. A P=O peak is shown at 1144.491 cm^{-1}. Both the MWCNTs-TBP and the MWCNTs-TBP polymer spectra prove presence of the phosphate. However, the polymer has an additional amide peak at 1712.794 cm^{-1} because of polymerisation using TDI.

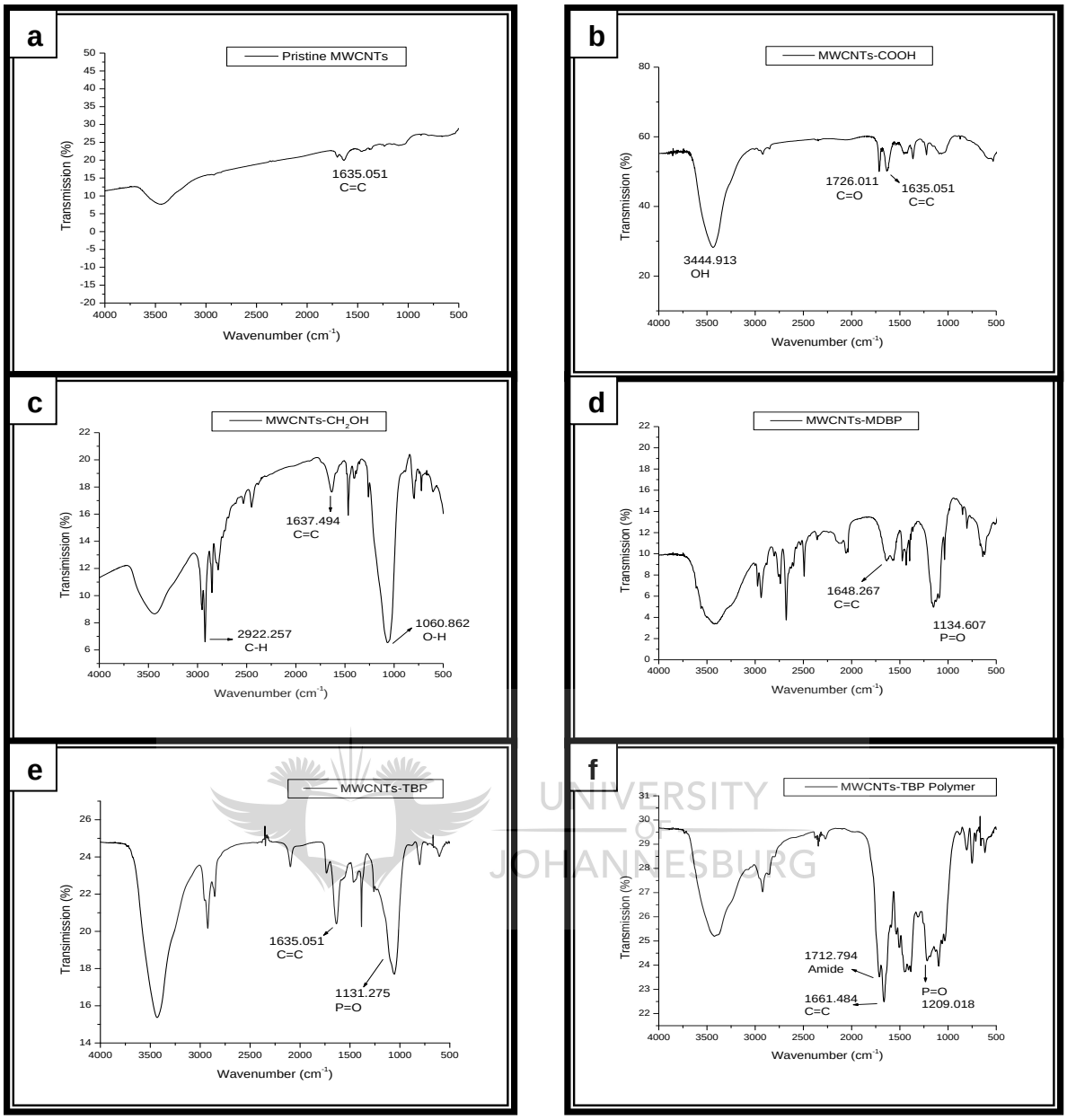

Figure 4.3: The FTIR spectra a) Pristine MWCNTs b) MWCNTs-COOH c) MWCNTs-CH_2OH d) MWCNTs-MDBP e) MWCNTs-TBP and f) MWCNTs-TBP polymer.

4.5 Raman

Figure 4.4 shows the effect of functionalisation in the structures of the MWCNTs by Raman spectroscopy. Raman scattering result in the formation of two significant peaks which are called; the disorder peak (D-band) and the graphite peak (G-band).[6] The ratio I_D/I_G gives the graphitisation degree of the carbons of

the MWCNTs.[6] The spectra demonstrate the D-bands at around 1350 cm^{-1} and the G-bands at around 1580 cm^{-1}. **Table 4.1** listing the I_D/I_G ratios of the different samples of MWCNTs proves the retainment of the graphitic arrangements of the MWCNTs because the values are less than one.

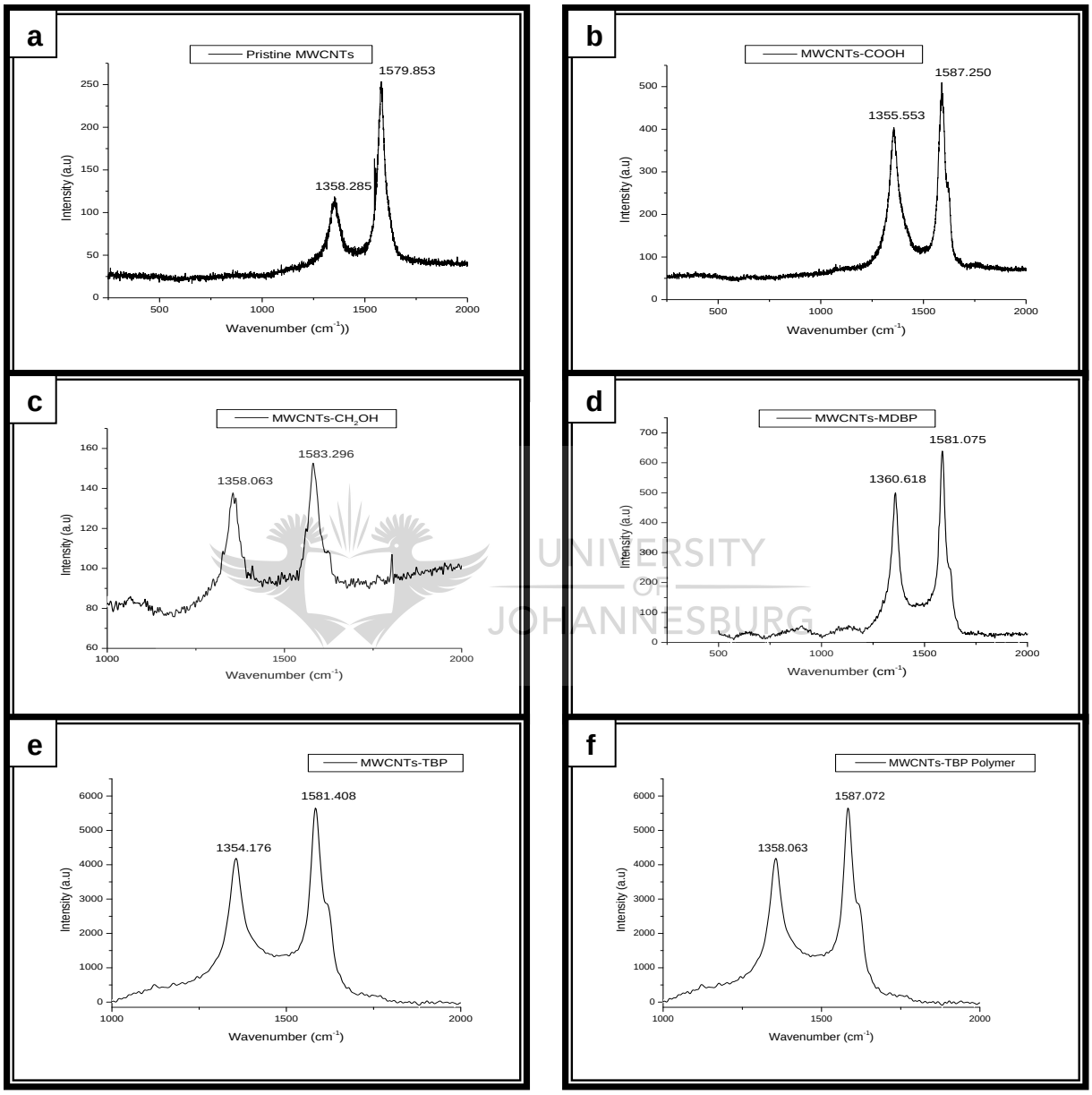

Figure 4.4: Raman a) pristine MWCNTs b) MWCNTs-COOH c) MWCNTs-CH_2OH d) MWCNTs-MDBP e) MWCNTs-TBP and f) MWCNTs-TBP polymer.

Table 4.1: Index for the graphitisation degree of the MWCNTs

Sample	I_D/I_G
Pristine MWCNTs	0.5
MWCNTs-COOH	0.8
MWCNTs-CH_2OH	0.8
MWCNTs-MDBP	0.8
MWCNTs-TBP	0.7
MWCNTs-TBP polymer	0.8

4.6 Thermo Gravimetric Analysis

Figure 4.5 gives the comparison of TGA spectra for pristine MWCNTs, MWCNTs-COOH, MWCNTs-CH_2O, MWCNTs-MDBP, MWCNTS-TBP and MWCNTs-TBP polymer. Degradation of the pristine MWCNTs is within the range 549 and 721 °C. About 89 % of the pristine MWCNTs were consumed. A maximum of 92 % MWCNTs-COOH were decomposed. The first 13 % weight loss at the range 216-350 °C is degradation of amorphous carbon. Within the range 366-728 °C, 79 % weight loss, COOH functional groups decomposed.

The MWCNTs-CH_2OH plot show 3 stages of degradation. The first one between 216-294 °C showing a 49 % weight loss is amorphous carbon degradation. Datsyuk *et al* (2008) confirms that amorphous carbon tends to be oxidised at temperatures below 500 °C.[1] The second section between 293 and 590 °C with 20 % weight loss is due to elimination of the hydroxyl groups. Datsyuk *et al* (2008) suggests that hydroxyl functions degrade between 350 and 500 °C.[1] The weight loss of 26 % within 590-683 °C is the decomposition of MWCNTs` skeleton. About 97 % of the MWCNTs-CH_2OH decomposed within the temperature ranges discussed.

The MWCNTs-MDBP`s amorphous carbon was decomposed within 164 and 245 °C and 65 % weight was lost. The methylene dibutyl phosphate (MDBP) decomposed between 245 and 773 °C at 14 % weight loss. In a study by Ndzimandze (2007)[7] conducted in our laboratory, the degradation of a phosphorylating compound was observed at 628 °C, which is in line with our degradation range of the MDBP. Approximately 96 % of the MWCNTs-MDBP degraded.

The MWCNTs-TBP decomposed in the range 155 and 660 °C. The first degradation within the range of 155-273 °C is removal of amorphous carbon. This range has 8 % weight loss. The range (454-554 °C) is the decomposition of hydroxyl functions with 11 % weight loss. Tributyl phosphate degraded within 561 and 660 °C with a percentage weight loss of 25 %. Approximately 47 % of the MWCNTs-TBP decomposed. **Fig. 4.6** shows the derivative plot for the MWCNTs-TBP.

About 97 % of MWCNTs-TBP polymer was burnt. Moisture decomposed between 45 and 142 °C and had a percentage weight loss of 6 %. The range (180-245 °C) with 7% weight loss is amorphous carbon degradation. Amide functions` degraded between 259 and 363 °C. Hydroxyl functions decomposed between 377 and 522 °C. Finally the TBP`s degradation occurred within 589 and 777 °C with a 37 % weight loss. A derivative plot for the MWCNTs-TBP polymer is shown in **Fig. 4.6**. **Table 4.2** summarises the degradation temperature ranges of the six samples of MWCNTs.

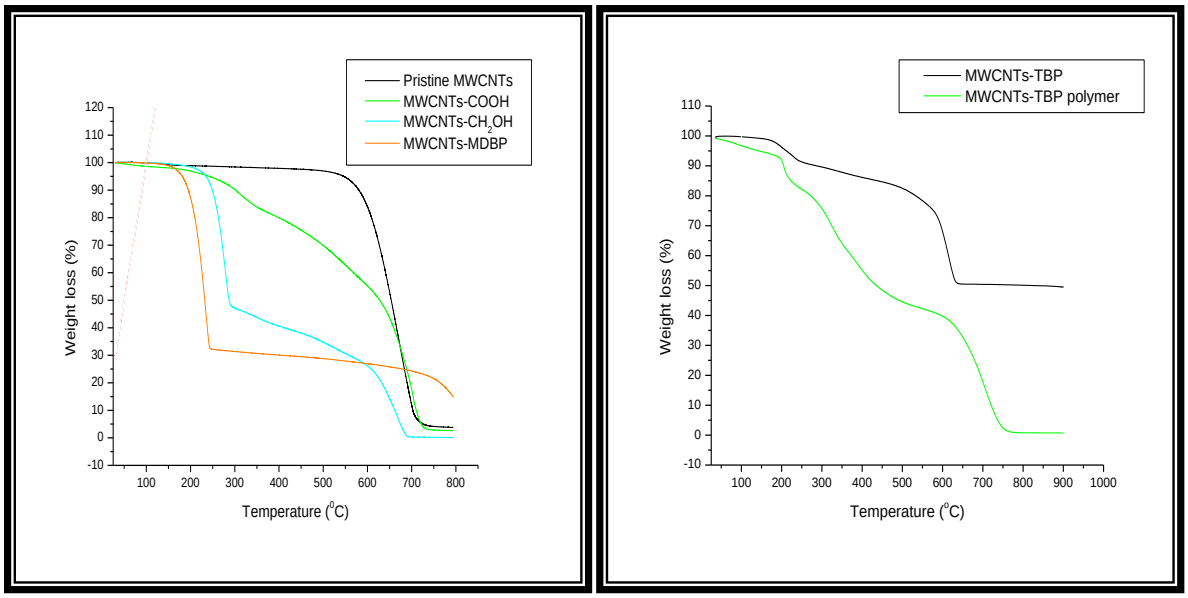

Figure 4.5: TGA for Pristine MWCNTs, MWCNTs-COOH, MWCNTs-CH_2OH MWCNTs-MDBP, MWCNTs-TBP and MWCNTs-TBP polymer.

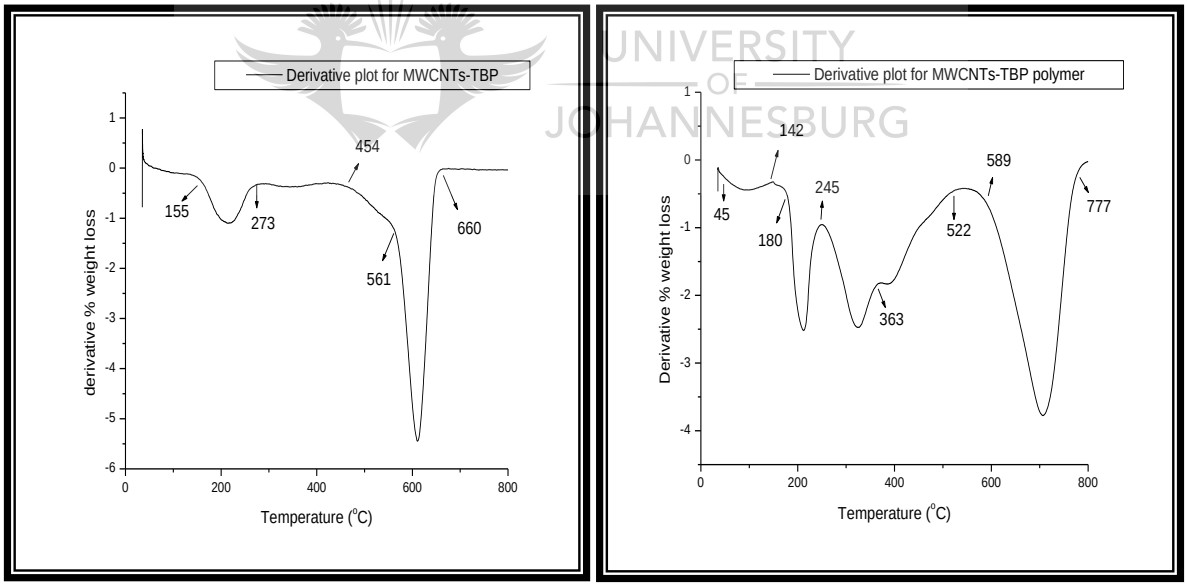

Figure 4.6: Derivatives plots for MWCNTs-TBP and MWCNTs-TBP polymer

Table 4.2: Thermal stability of the pristine MWCNTs, MWCNTs-COOH, MWCNTs-CH_2OH, MWCNTs-MDBP, MWCNTs-TBP and MWCNTs-TBP polymer.

Sample	Initial degradation Temp (°C)	Final degradation Temp (°C)
Pristine MWCNTs	549	721
MWCNTs-COOH	216	728
MWCNTs-CH_2OH	216	683
MWCNTs-MDBP	164	791
MWCNTs-TBP	155	660
MWCNTs-TBP Polymer	45	777

4.7 Energy dispersive X-ray Spectrometry

Fig. 4.7 and 4.8 illustrates the EDX for pristine and functionalised MWCNTs**.** Carbon is prominent in all the spectra and this is because it is the main constituents for CNTs. **Fig. 4.7 (a)** has traces of iron that are remains from the catalyst used in the synthesis of the MWCNTs. After oxidation, **Fig. 4.7 (b)** shows inclusion of oxygen proving the attachment of the carboxylic functions to the tubes. MWCNTs-MDBP (**Fig. 4.8 (a)**), MWCNTs-TBP (**Fig. 4.8 (b)**) and MWCNTs-TBP polymer (**Fig. 4.8 (c)**) have a phosphorus peak which confirms the incorporation of the phosphates to the MWCNTs.

Use of vacuum silicon grease to grease the apparatus introduced silicon to the MWCNTs in **Fig. 4.8 (a-c)**. However, It is not observed in **Fig. 4.7 (a-b)** because the pristine and MWCNTs-COOH were only exposed to either no vacuum grease or very little during the synthesis, purification and oxidation unlike the acylation, amidation and reduction processes. An inert atmosphere was utilised to conduct

the three latter processes. Therefore, more silicon vacuum grease was used to grease the apparatus. These processes were subject to longer reflux durations as compared to the purification and oxidation (i.e. 5 days for amidation of the MWCNTs) which increased the chances of the contamination by the silicon vacuum grease. During the oxidation of the CNTs, both COOH and OH functions attached to the MWCNTs. With subjection to more functionalisation: acylation, amidation and reduction the COOH were changed to hydroxyl functions. However, the OH were chlorinated which explains the presence of chlorine in **Fig. 4.8 (a-c)**. The aluminium peak was peaked from the background or stage of the instrument.

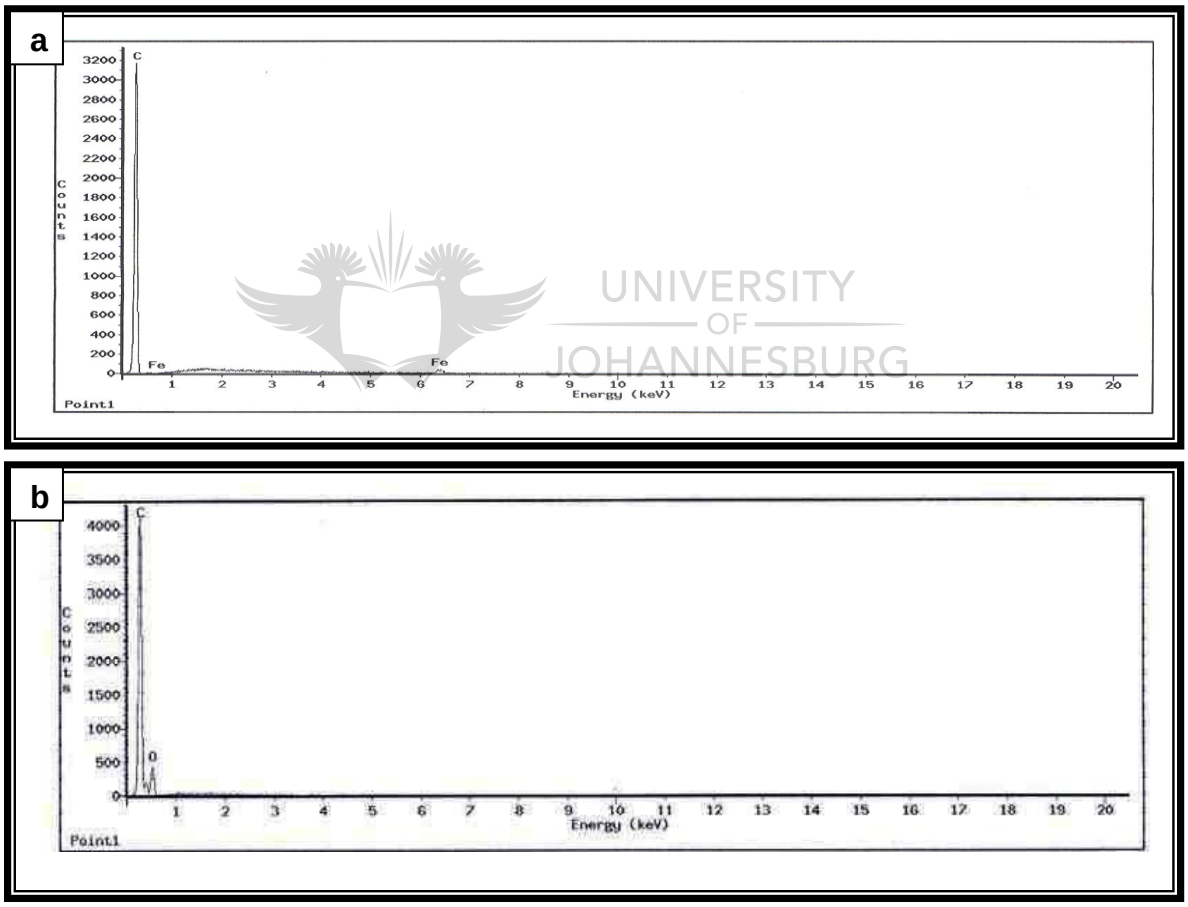

Figure 4.7: EDX a) Pristine MWCNTs b) MWCNTs-COOH

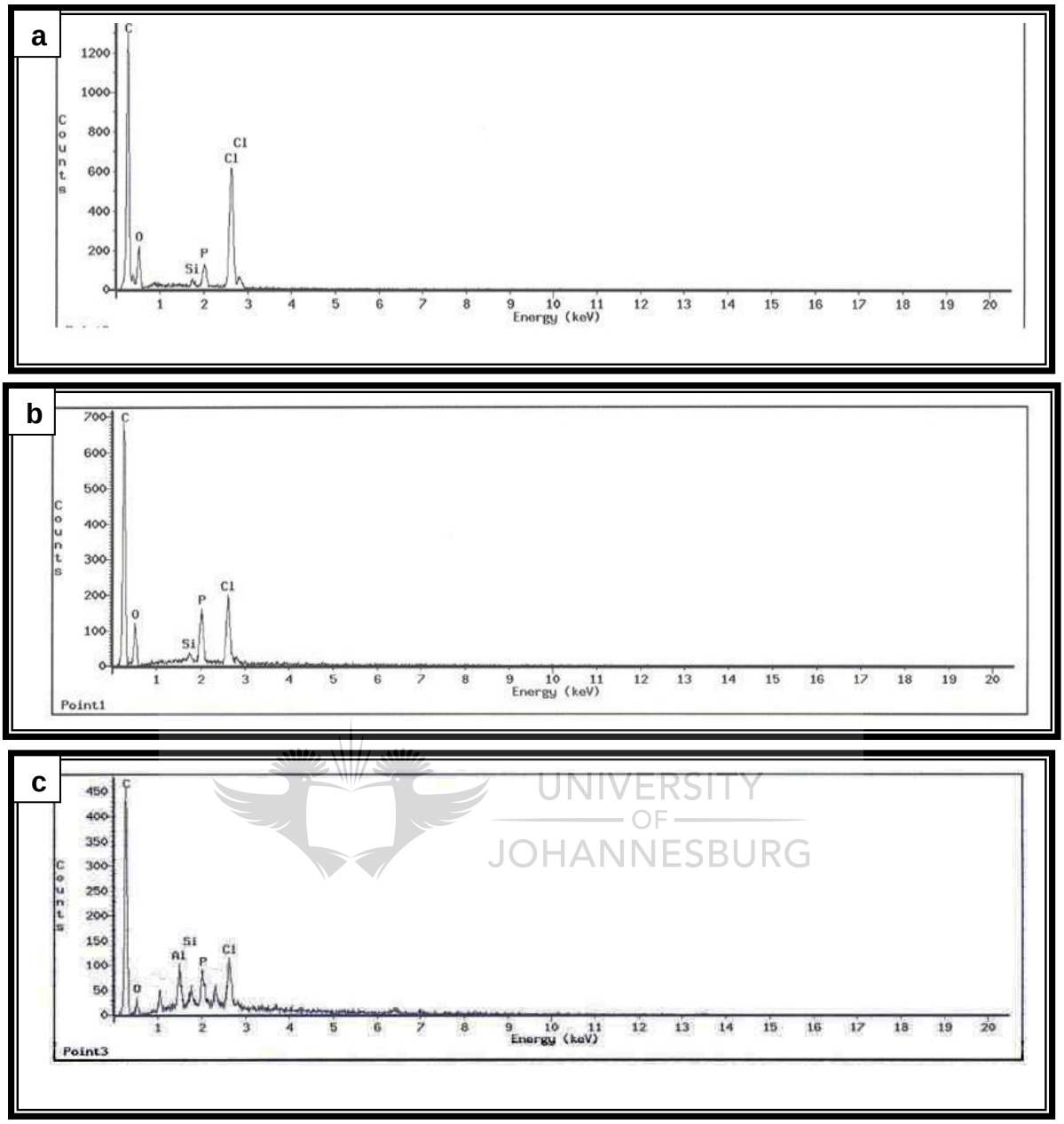

Figure 4.8: a) EDX MWCNTs-MDBP b) MWCNTs-TBP c) MWCNTs-TBP polymer

4.8 Scanning X-ray photoelectron Spectroscopy

The SXPS shown in **Figure 4.9** have a high carbon atomic concentration of 93.5 % that is because of the C-C and C-O bonds. The C-C bond is the constituent for the MWCNTs and the C-O is from the methylene dibutyl phosphate. Silicon (0.5 % atomic concentration) is from the silicon vacuum grease. The 0.2 % atomic concentration of P is due to the P=O bond from the methylene dibutylphosphate.

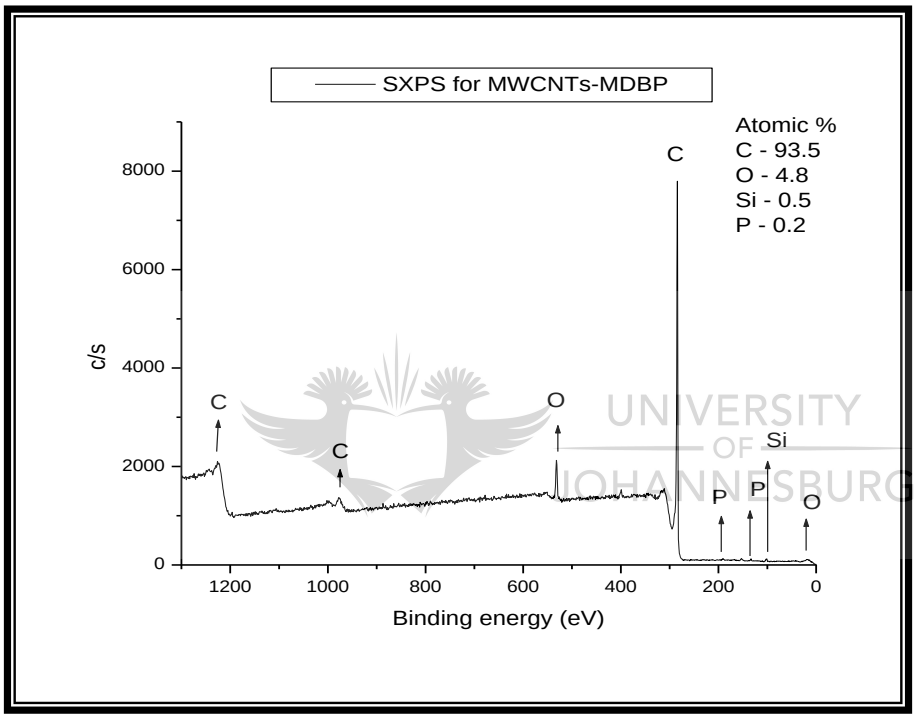

Figure 4.9: SXPS for MWCNTs-MDBP.

Figure 4.10 (SXPS for MWCNTs-TBP polymer) shows presence of the following elements; carbon, oxygen, nitrogen and phosphorus. The 82.1 % of carbon is because of the MWCNTs skeleton (C-C) and the P-O and C-O bonds explain the 17 % oxygen. The.4 % P is from the P-O bonds. However, phosphorus has the least percentage. This proves that least amount of TBP was incorporated to the MWCNTs. Nitrogen (0.5 %) is because of the N-MWCNTs bond as shown in **Scheme 3.10** of chapter 3. During the synthesis of MWCNTs-TBP, nitrogen forms the link between MWCNTs and TBP.

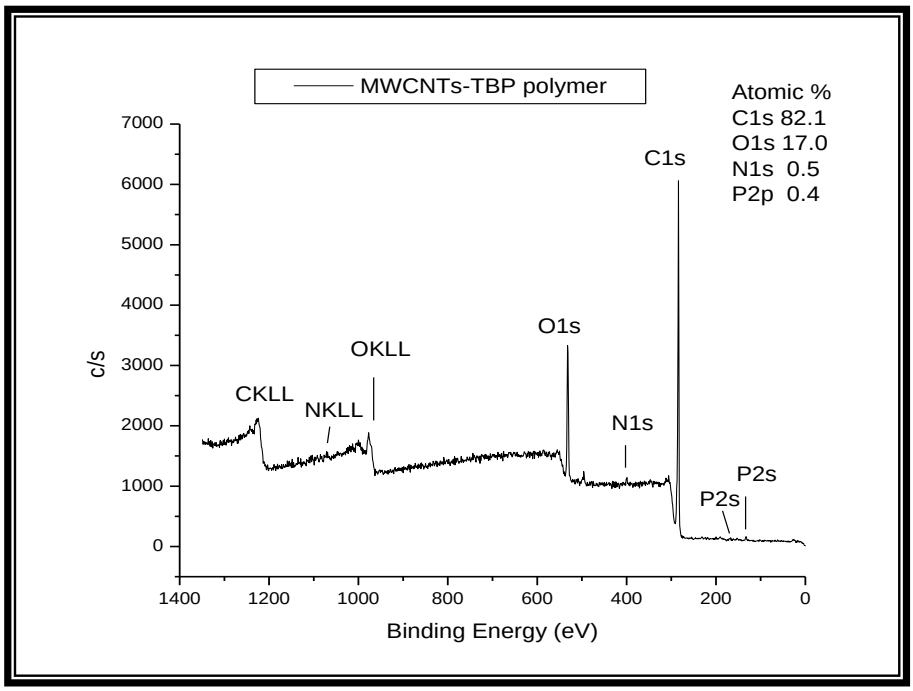

Figure 4.10: SXPS for MWCNTs-TBP polymer

4.9 Brunauer Emmet-Teller

Functionalisation influenced the surface area of the MWCNTs thereby influencing the average pore volume and pore diameter of the MWCNTs samples (**Table 4.3**). The pristine-MWCNTs have a surface area of 39.1 m^2/g and a rapid increase of the surface area after the introduction of the carboxylic and hydroxyl functions is observed. The average pore volumes for both the MWCNTs-COOH and MWCNTs-CH_2OH when compared with the pristine MWCNTs increased from 0.15 cm^3/g to 0.30 and 0.28 cm^3/g respectively. The surface area of the phosphorylated MWCNTs (MWCNTs-MDBP, MWCNTs-TBP and the polymer) is comparable with that of the pristine MWCNTs (slight decrease from the pristine MWCNTs surface area). Their average pore volume and pore diameter follows suit by being comparable to the pristine MWCNTs.

Table 4.3: BET results for the different MWCNTs samples

Sample	**Surface area** (m^2/g)	**Average pore volume** (cm^3/g)	**Average pore diameter** (nm)
Pristine MWCNTs	39.1	0.15	15.1
MWCNTs-COOH	73.7	0.30	16.1
MWCNTs-CH_2OH	80.1	0.28	13.9
MWCNTs-MDBP	32.57	0.16	13.1
MWCNTs-TBP	33.45	0.16	13.3
MWCNTs-TBP polymer	35.56	0.18	13.4

4.10 Application of the MWCNTs samples in radioactive waste treatment

Uranium (U) exists in various unique chemical forms.[8] In nature, it exists as an oxide. An oxidised form of uranium is found in soil whereas in water usually as a uranyl hydroxyl complex.[8] Uranium oxide (UO_2) is predominately used for nuclear reactor fuel.[8] Soil properties such as oxidation-reduction potential, pH, concentration of complexing anions, soil porosity, soil particle size and sorption properties and the amount of water available influences the mobility of uranium in soil and its leaching to ground water.[8] Uranium can exists in the $^{+}3$, $^{+}4$, $^{+}5$ and $^{+}6$ oxidation states. However, in aqueous media only U(IV and U(VI) are stable. The abiotic and biological processes transporting U in the soil converts U(VI) (soluble) to U(IV) that is insoluble.[9] This oxidation-reduction reaction has received major attention because it has an important effect on the mobility of U in the natural environment.[8] In solution U exist predominately as UO_2^{2+} and as soluble carbonate complexes $(UO_2)_2CO_3(OH)^{3-}$, $UO_2CO_3^{0}$, $UO_2(CO_3)_2^{2-}$, $UO_2(CO_3)_3^{4-}$ and

$(UO_2)_3(CO_3)_6^{6-}$.[10] A hydrolysed form of U(VI) is found in soil (pH 4.0 to 7.5). U(IV) is stable under reducing conditions, and it is considered immobile.[8]

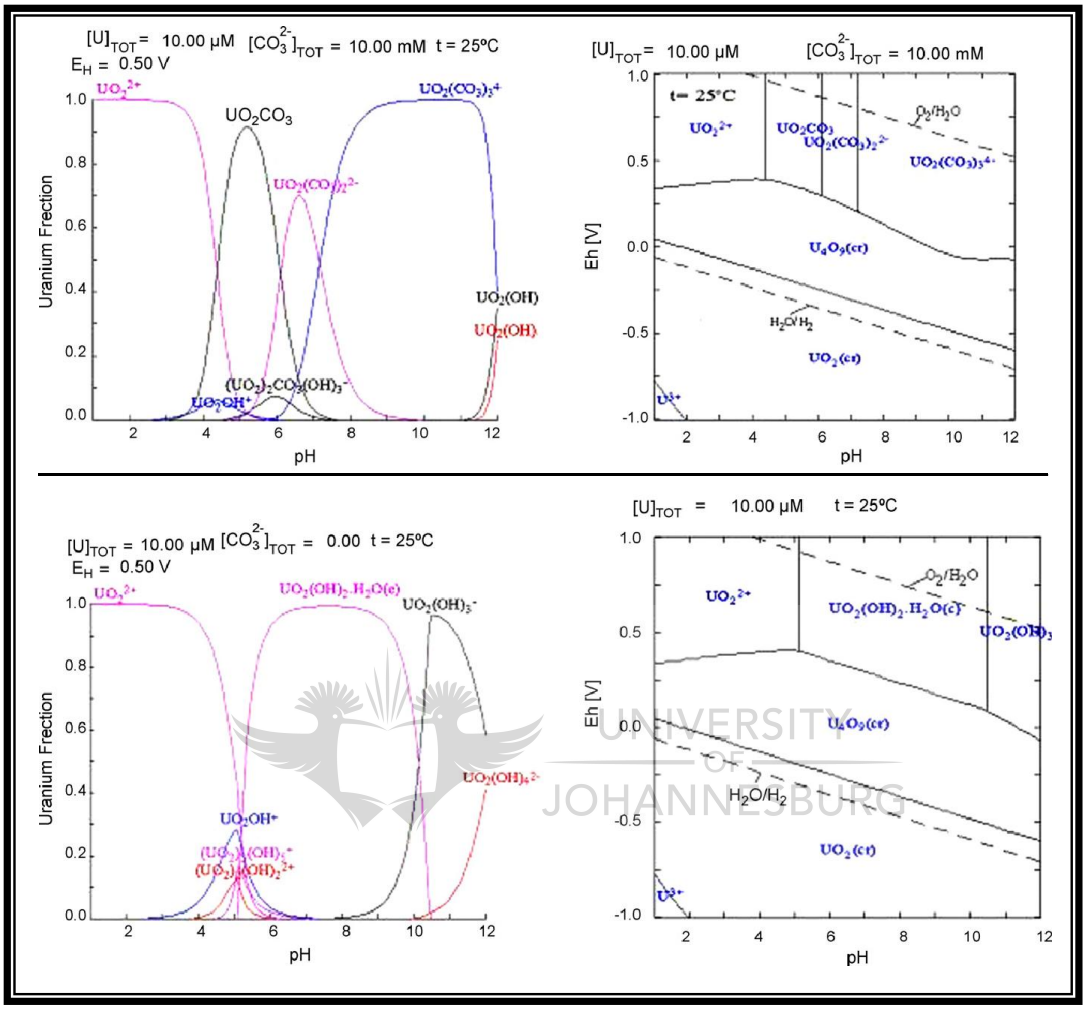

Figure 4.11: Eh-pH and uranium species distribution as a function on pH for oxidising-reducing conditions.[11]

A thermodynamic data is used in the estimation of the solubilities and speciation of U. Presence of inorganic ligands in ground water such as $[OH]^-$, $[HCO_3]^-$, $[CO_3]^{2-}$, $[H_2PO_4]^{2-}$, $[PO_4]^{3-}$, $[SO_4]^{2-}$ is taken into consideration.[12] **Figure 4.11** shows the thermodynamic stability areas for different U species in aqueous solutions for both closed and open systems. In the open system U(IV) is insoluble and immobile and forms uraninite (UO_2) whereas U(VI) which is soluble and mobile forms soluble complexes with carbonate anions in natural water. A series of strong anionic aqueous carbonate complexes dominates the aqueous speciation of U(VI) in carbon containing water at neutral and basic higher pH. For example

$[UO_2(CO_3)_2]^{2-}$ is found between pH 7 and 8 in an oxidised environment (**Fig. 4.11**).[8] Research has proven that carbonate complexing reduces adsorption of uranium resulting in its release from the soil.[13] At low Eh the solid phase of uranium and dissolved uranium carbonate complexes results. At Eh values above 0.25 V and pH (7-8), (1-5) uranium (VI) exists as uranyl ion $[UO]^{2+}$. Carbonate ligands plays a major role in alkaline medium and it causes the solubility of U(VI).[8]

In the closed system, the stability field of the U(VI) is altered by the formation of the carbonate complexes.[8] Uranyl complexes such as $UO_2(OH)^+$ and $(UO_2)_3(OH)_5^+$ are also formed except that they are formed only in small amounts in high temperatures.[8] In reducing waters hydrolysis of U(IV) forms $U(OH)_4^0$. The reduced uranium hydrolysis forming colloids because it solubility is lowered as the environmental conditions are altered. However, the colloids formation is hindered by the high concentrations of inorganic salts.[8]

The distribution coefficient (K_d) value is a guide to determine the possibility of using the MWCNTs for the adsorption of radioactive elements from liquid waste streams. Uranium extraction from radioactive liquid waste using the MWCNTs is summarised in **Table 4.4**. The performance of the MWCNTs in uranium adsorption gave very low K_d values. The MWCNTs-MDBP gave a K_d value of 8.5 mL/g which is higher than all its counterparts but nonetheless the MWCNTs failed to adsorb uranium. The MWCNTs-TBP polymer was expected to adsorb more uranium from the liquid waste because TBP is used in uranium adsorption. Several factors must have contributed to the poor performance of the MWCNTs. The presence of more chlorine than the phosphorus peak as shown by the EDX in **Fig. 4.8** could have hindered attachment of more phosphates (TBP) to the MWCNTs. The presence of the Phosphorus peak proves the presence of the phosphates but the quantity is very little as shown by the SXPS (**Fig. 4.9 and 4.10**). The BET results (**Table 4.3**) shows that the surface area, average pore volume and diameter of the phosphorylated MWCNTs are comparable to those of pristine MWCNTs. This observation proves not much TBP attached to the MWCNTs. **Fig. 4.1 (d-f)** illustrates the phosphorylated MWCNTs clustered together. The adhering of the tubes together must have hindered adsorption of

uranium by failure to expose the less TBP to the waste. For example, **Fig. 4.2 (e)** shows TBP entangled between CNTs.

Table 4.4: The K_d values of uranium extraction by MWCNTs samples

MWCNTs samples	**K_d values (mL/g)**	
	Basic medium (1M Na_2CO_3)	**Acidic medium (1 M HNO_3)**
Pristine-MWCNTs	3.8	2.5
MWCNTs-COOH	Not clear	3
MWCNTs-MDBP	1.5	8.5
MWCNTs-TBP polymer	Not clear	0

In order to determine if MWCNTs have potential to extract radionuclides from radioactive solutions, the possible extraction of iodine-131 was determined. Pristine-MWCNTs, MWCNTs-COOH and MWCNTs-MDBP were compared with SWCNTs and double walled carbon nanotubes (DWCNTs). The same uranium extraction methodology was used for iodone-131 extraction and results are shown in **Table 4.5**. The SWCNTs gave the highest K_d values of 81694.86, 509.51 and 2829.59 mL/g in pH 3, 7 and 10 respectively.

The DWCNTs at pH 3 has a K_d value of 2405.23 mL/g also proved to be good adsorbent for the iodine-131. The MWCNTs did not extract iodine-131 as indicated by the low K_d values. However, their performance in iodine-131 extraction showed improvement when compared with uranium extraction and the MWCNTs-MDBP gave the highest K_d values when compared with the other MWCNTs samples. This result therefore indicates that increase in the number of graphite walls of the CNTs decreases the K_d values. When comparing the adsorption characteristics of the SWCNTs with those of graphite powder (**Table 4.5**), the results clearly indicates the advantages of using CNTs with high

surface area than powder for the extraction of iodine. The possibility therefore exists that nanotechnology is a potential tool for the removal of radionuclides from radioactive waste streams.

Table 4.5: The K_d values for iodine extraction by the Carbon materials

Samples	**K_d values (mL/g)**		
	pH **3**	**7**	**10**
Graphite	7.10	1.35	1.10
Pristine-SWCNTs	**81694.86**	**509.51**	**2829.59**
Pristine-DWCNTs	**2405.23**	30.15	55.67
Pristine-MWCNTs	52.17	38.42	22.40
MWCNTs-COOH	5.68	27.73	13.91
MWCNTs-MDBP	**126.52**	**101.33**	**105.29**

4.11 Conclusion

The phosphorylation of the MWCNTs was successfully as proven by the FTIR, EDX and SXPS spectra that show presence of phosphorus. The morphology of the different MWCNTs was studied by the SEM and TEM. These techniques show changes in morphology of the CNTs, it is notable that after inclusion of the phosphates the tubes clustered together. The adhering of the tubes to one another hindered the exposure of the phosphates and lowered the surface area of the MWCNTs as proven by the BET analysis.

The phosphorylated MWCNTs did not absorb uranium as expected. This could be because their surface area was comparable to the pristine MWCNTs meaning that attachment of enough TBP is questionable. The SXPS proves that minimum percentages of the phosphates were observed from the MWCNTs. Impurities

such as chlorine and silicon could have hindered more phosphate from attaching to the MWCNTs. Pristine SWCNTs showed greater adsorption potential when they were able to adsorb iodine from radioactive waste streams.

References:

1. V. Datsyuk; M. Kalyva; K. Papagelis; J. Parthenious; D. Tasis; A. Siokou; I. Kallitsis and C. Galiotis. Chemical oxidation of multiwalled carbon nanotubes. *Carbon*. **46** (2008) 833-840.

2. Y. Wang; Z. Iqbal and S.V. Malhotra. Functionalisation of multiwalled carbon nanotubes with amines and enzymes. *Chemical Physics Letters.* **402** (2005) 96-101.

3. X. Tan; M. Fang; C. Chen; S. Yu and X. Wang. Counterion affects of nickel and sodium dodecylbenzene sulfonate adsorption to multiwalled carbon nanotubes in aqueous solution. *Carbon*. **46** (2008) 1741-1750.

4. E. Cho; S. Shin and Y. Yoon. First-principle studies on carbon nanotubes functionalized with azomethine ylides. *Journal of physical Chemistry C*. **112** (2008) 11667-11672.

5. L. Peng and T. Wang. Ultrasonic-assisted chemical oxidative cutting of multiwalled carbon nanotubes with ammonium persulfate in neutral media. *Applied Physics A*. **97** (20090 771-775.

6. C. Yang; X. Hu; D. Wang; C. Dai; L. Zhang; H. Jin and S. Agathopoulos. Ultrasonically treated multi-walled carbon nanotubes (MWCNTs) as PtRu catalyst supports for methanol electrooxidation. *Journal of power sources*. **160** (2006) 187-193.

7. Ndzimandze TM. Phosphorylation of multiwalled carbon nanotubes. University of Johannesburg, MSc Dissertation, 2007.

8 . M. Gavrilescu; L. V. Pavel; I. Cretescu. Characterisation and remediation of soils contaminated with uranium. *Journal of hazardous Materials*. **163** (2009) 475-510.

9 . M.D. Campbell and K. T. Biddle. Frontier areas and exploration techniques. Frontier uranium exploration in the South-central United states, in M.D. Campbell. Geology of alternative energy resources. Houston geological society. Houston Tx. (1997) 3-44.

10 . L. Ciavatta; D. Ferii; I. Genthe and F. Salvatore. The first acidification step of the tris(carbonato)dioxourantantate(VI)ion, $UO_2(CO_3)_3^{4-}$. *Journal of Inorganic Chemistry*. **20** (1981) 463-467.

11 . A. Ikeda; S. Tsushima; K. Takao; Y. Ikeda, A.C. Scheinost and G. Bernhard. A comparative study of U(VI) and U(V) carbonato complexes in aqueous solution. *Journal of Inorganic Chemistry*. **46** (2007) 4212-4219.

12 . M. Dozol; R. Hagemann. Radionuclide migration in groundwaters, review of the behavior of actinides. *Pure Applied Chemistry*. **65** (1993) 1081-1102.

13 . T.D. Waite; J.A. Davis; T.E. Payne; G.A.Waychunas and N. Xu. Uranium(VI) adsorption to ferrihydrite. Application of a surface complexation model, Geochim. Cosmochim. *Acta.* **58** (1994) 5465–5478.

CHAPTER 5

CONCLUSIONS AND RECOMMENDATIONS

5.1 Conclusions

- The synthesis, purification and functionalisation of the multiwalled carbon nanotubes were successful and proven by the characterisation techniques used.

- The synthesis of the phosphorylated compounds; methylene dibutyl phosphate and tributyl phosphate was attained as proven by the NMR analysis in chapter 4.

- The synthesis of the MWCNTS-MDBP and MWCNTS-TBP polymer was successfully achieved as verified by the FTIR, SXPS and EDX which showed presence of phosphorus in the MWCNTs.

- The adsorption of uranium by the current MWCNTs samples was not successful. A minimum amount of the phosphate was attached to the MWCNTs as proven by the SXPS and this hindered adsorption of uranium. The EDX also showed presence of Cl that could have hindered attachment of more phosphate to the MWCNTs. The surface area and average pore volume and diameter of the phosphorylated MWCNTs are analogous to those of pristine MWCNTs, which indicate that incorporation of the phosphate to the MWCNTs was not enough although the EDX and SXPS do show its presence. The adherence of the MWCNTs-TBP polymer's tubes together shown by the SEM and TEM could also have hindered the exposure of the phosphate to the uranium.

- When comparing the MWCNTs with SWCNTs and DWCNTs in iodine-131 extraction they extracted the least amount of iodine. The

SWCNTs extracted the most followed by the DWCNTs then the phosphorylated MWCNTs. The lesser the number of CNTs walls the larger the K_d value. The number of walls of the CNTs influenced the adsorption of iodine-131 as SWCNTs performed much better than the MWCNTs and DWCNTs.

- The study aimed at exploring the possibility of utilising nanotechnology in the removal of radionuclides from waste streams. Nonetheless, the poor performance of the MWCNTs-TBP in uranium adsorption did not rule out that possibility.

5.2 Recommendations

- Uses of phosphorylated SWCNTs (p-SWCNTs) for Uranium extraction as the pristine-SWCNTs have such great potential. Incorporating the phosphate to the SWCNTs can help to achieve our objective that was to solidify the radioactive waste because the SWCNTs have proven from the iodine testing to have large surface area exposed for absorption.

- The MWCNTs-TPB polymer can be unclustered to expose all the layers to the uranium. Sonication in a solvent before the analysis could help to disperse the tubes. Due to the clustering there is a possibility that only few of the phosphate groups were exposed to the radionuclide waste and therefore uranium adsorption was hindered. Dispersal of the tubes can aid in exposing all the phosphates groups to the radionuclide waste.

- Incorporation of more phosphates to the MWCNTs for the adsorption of radionuclides from waste streams can aid the adsorption of uranium.

APPENDIX

NMR AND FTIR SPECTRA

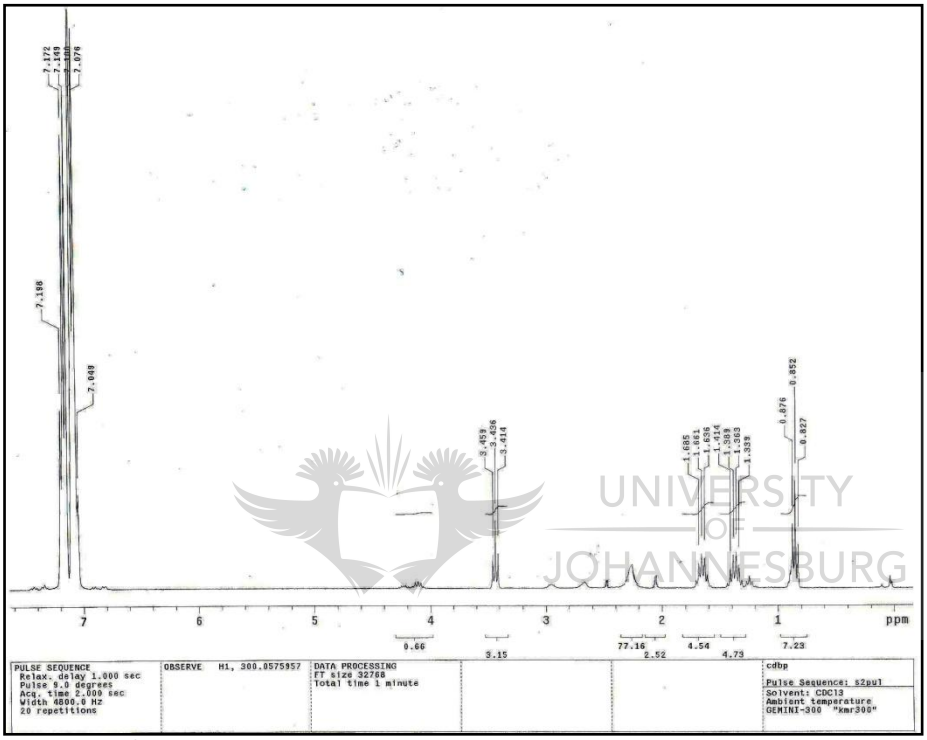

A 1: The ^{1}H NMR spectrum for dibutyl chlorophosphate

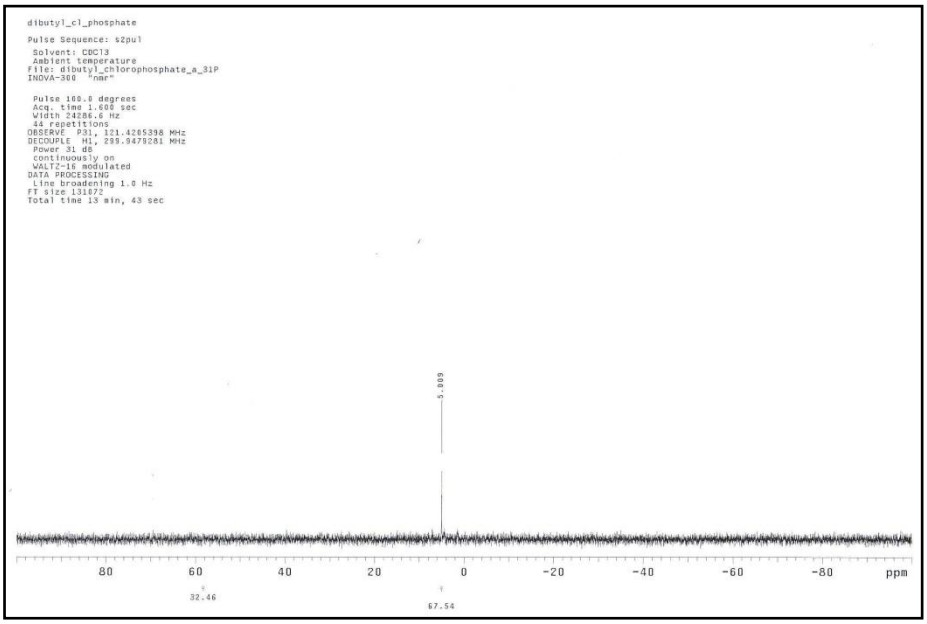

A 2: The ^{31}P NMR spectrum for dibutyl chlorophosphate

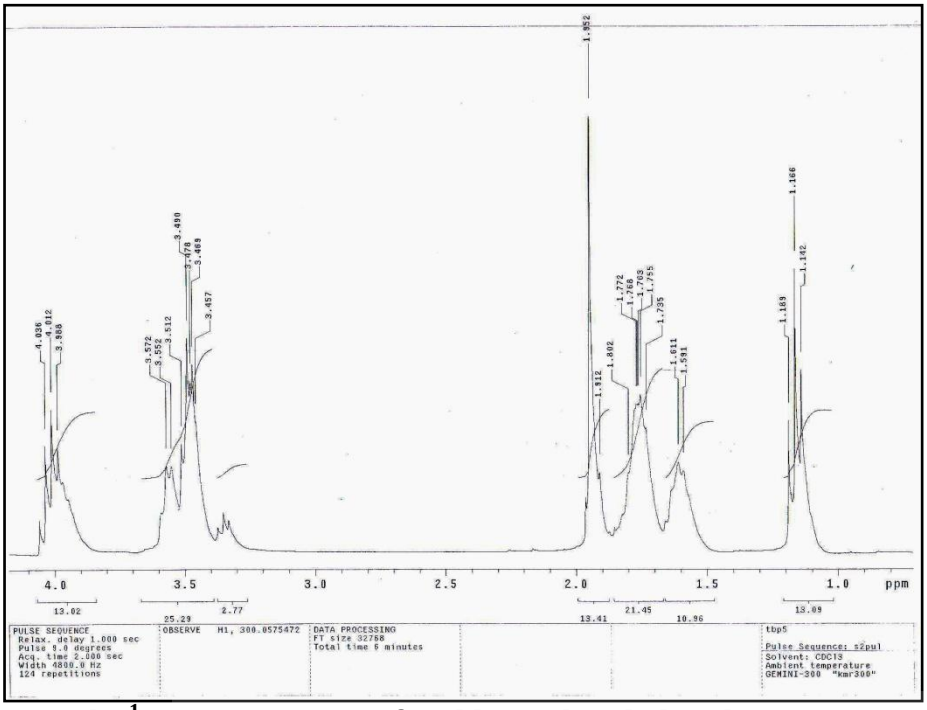

A 3: The ^{1}H NMR spectrum for chlorotributyl phosphate

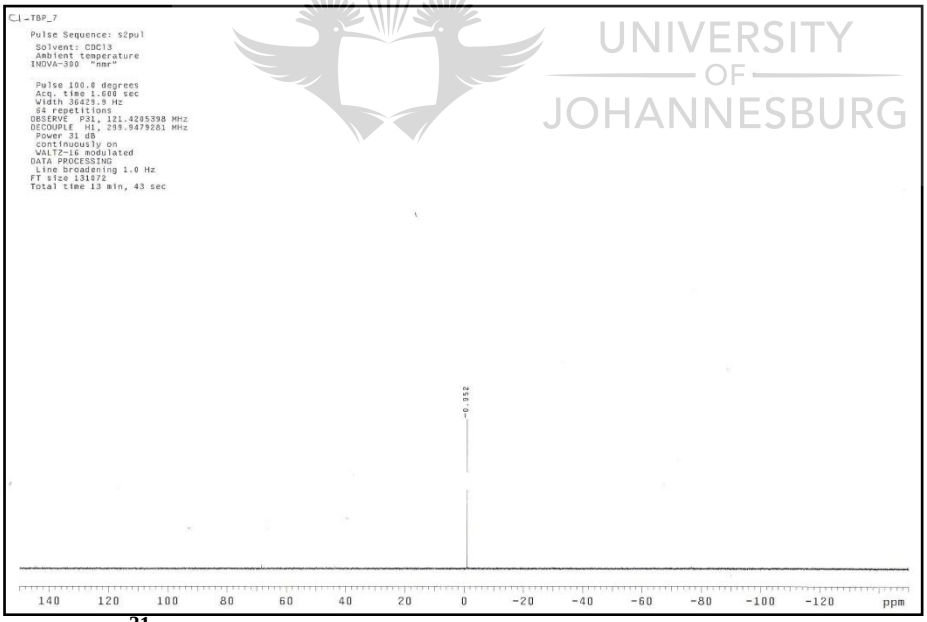

A 4: The ^{31}P NMR spectrum for chlorotributyl phosphate

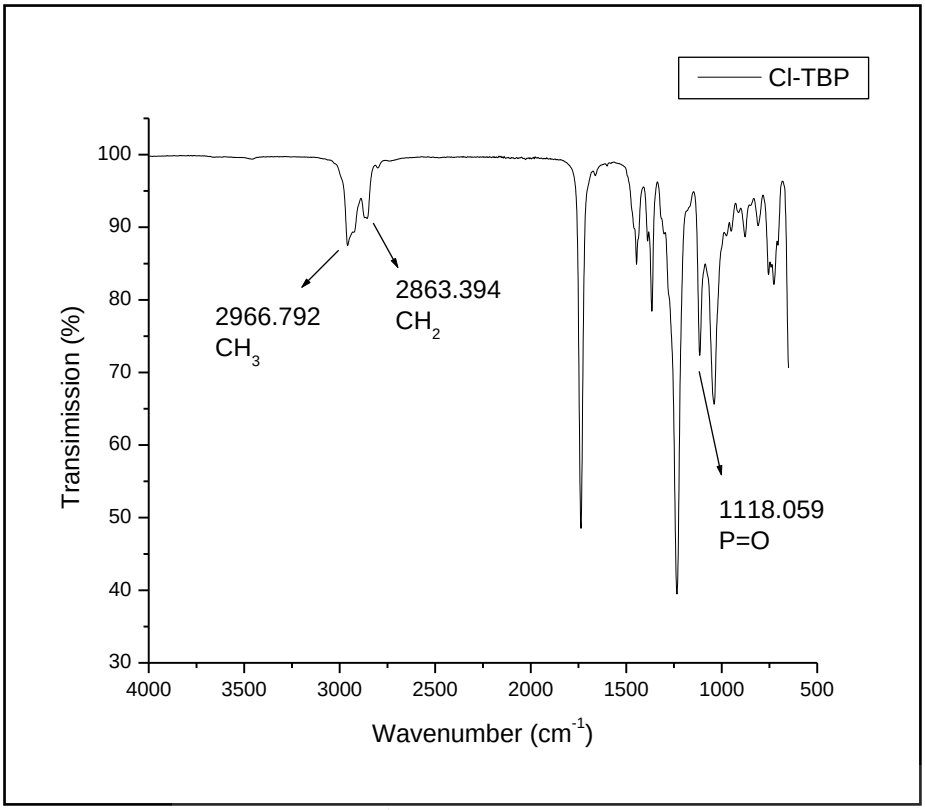

A 5: The FTIR spectrum for chlorotributylphosphate

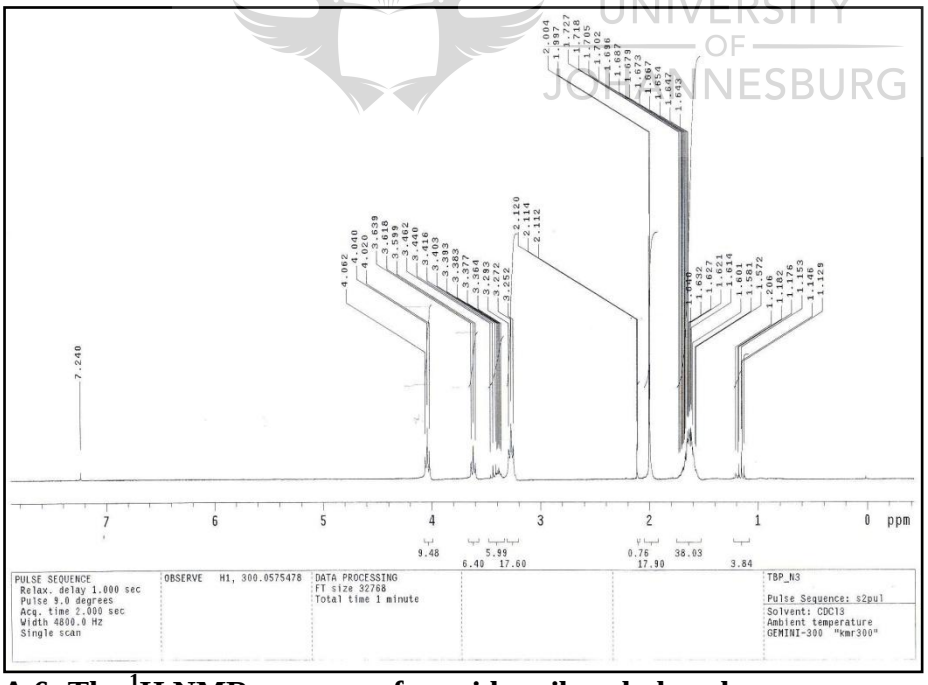

A 6: The ^{1}H NMR spectrum for azido-tributyl phosphate

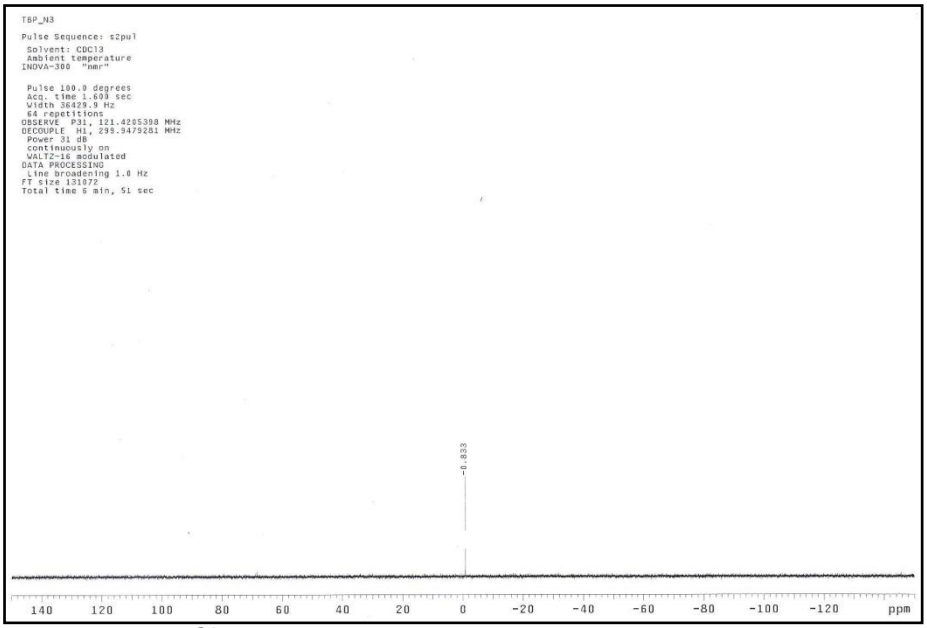

Figure 7: The ^{31}P NMR spectrum for azido-tributyl phosphate

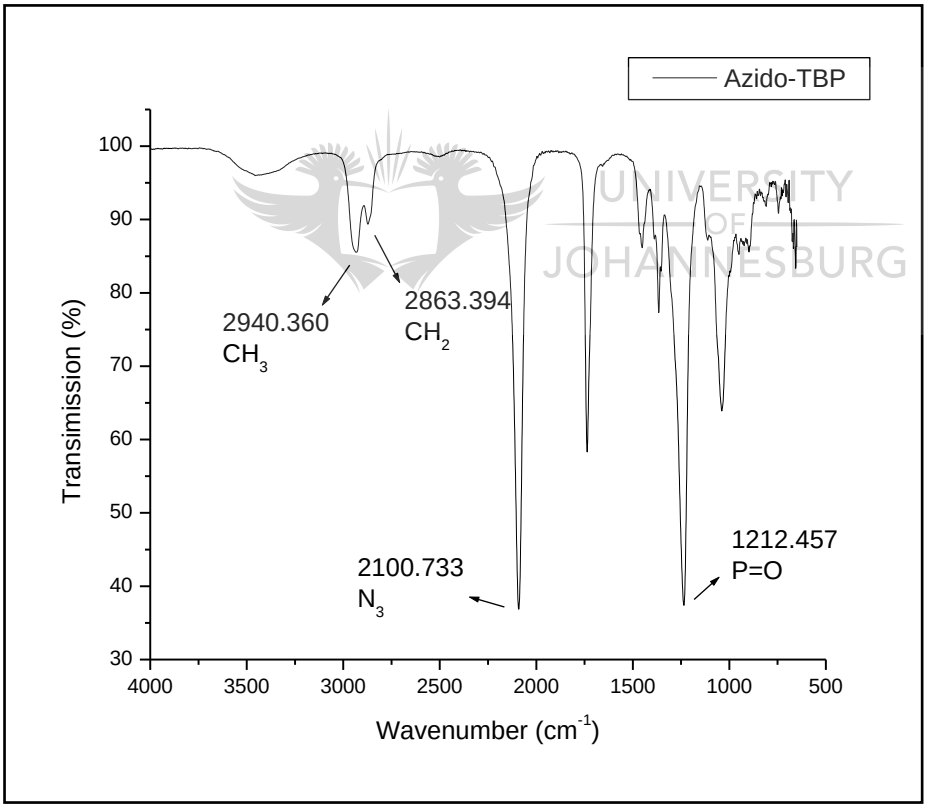

Figure 7: The FTIR spectrum for azido-tributylphosphate